Boletín de la Sociedad Española de Cerámica y Vidrio
Vol 53, 1, 1-14, Enero-Febrero 2014 ISSN 0366-3175. eISSN 2173-0431.
doi: 10.3989/cyv.12014

BOLETIN DE LA SOCIEDAD ESPAÑOLA DE
Cerámica y Vidrio
ARTICULO DE REVISIÓN

Synthesis, microstructure and properties of $BiFeO_3$-based multiferroic materials: A review

M. S. BERNARDO*

*Departmento de Electrocerámica, Instituto de Cerámica y Vidrio (CSIC), Kelsen, 5, 28049, Madrid, Spain.

$BiFeO_3$-based materials are currently one of the most studied multiferroics due to their possible applications at room temperature. However, among the large number of published papers there is much controversy. For example, possibility of synthesizing a pure $BiFeO_3$ phase is still source of discussion in literature. Not even the nature of the binary Bi_2O_3-Fe_2O_3 diagram has been clarified yet. The difficulty in controlling the formation of parasite phases reaches the consolidation step. Accordingly, the sintering conditions must be carefully determined both to get dense materials and to avoid bismuth ferrite decomposition. However, the precise conditions to attain dense bismuth ferrite materials are frequently contradictory among different works. As a consequence, the reported properties habitually result opposed and highly irreproducible hampering the preparation of $BiFeO_3$ materials suitable for practical applications. In this context, the purpose of the present review is to summarize the main researches regarding $BiFeO_3$ synthesis, microstructure and properties in order to provide an easier understanding of these materials.

Keywords: $BiFeO_3$, synthesis, sintering, ferroelectric properties, magnetic properties.

Síntesis, microestructura y propiedades de materiales multiferroicos basados en $BiFeO_3$: Una revisión

Los materiales basados en $BiFeO_3$ son en la actualidad uno de los multiferroicos más estudiados debido a sus posibles aplicaciones a temperatura ambiente. Sin embargo, entre la multitud de trabajos publicados referentes a estos materiales existe mucha controversia. Por ejemplo, la posibilidad de sintetizar una fase $BiFeO_3$ pura es aún objeto de discusión en la bibliografía y la naturaleza de los diagramas de fases del sistema Bi_2O_3-Fe_2O_3 aún no está clara. La dificultad para controlar las fases parásitas se extiende al proceso de consolidación por lo que las condiciones de sinterización deben ser cuidadosamente controladas para obtener materiales densos y al mismo tiempo evitar la descomposición de la ferrita. No obstante, las condiciones precisas para obtener materiales densos de $BiFeO_3$ son frecuentemente contradictorias entre los distintos trabajos. Como consecuencia, las propiedades descritas son a menudo discordantes y poco reproducibles impidiendo la preparación de materiales de $BiFeO_3$ adecuados para sus aplicaciones prácticas. En este contexto, el propósito de esta revisión es resumir las principales investigaciones en torno a la síntesis, microestructura y propiedades de los materiales de $BiFeO_3$ facilitando así la comprensión de los mismos.

Palabras clave: $BiFeO_3$, síntesis, sinterización, propiedades ferroeléctricas, propiedades magnéticas.

1. MULTIFERROIC MATERIALS

By definition single phase multiferroic materials are those that simultaneously present at least two of the so-called "ferroic" properties: ferroelectricity, ferromagnetism and ferroelasticity [1]. These properties lie in the presence of an electric polarization, magnetization or elastic deformation that can be switched hysterically by the action of an electric field, a magnetic field or stressing, respectively. Recently, the multiferroic term has been extended to materials with other magnetic orders like ferrimagnetism or antiferromagnetism [2] and even to a ferrotoroid order [3, 4].

Magnetoelectric multiferroics are one of the most interesting categories of multiferroic materials. In this kind of materials the coexisting properties of ferroelectricity and ferromagnetism (or ferrimagnetism or antiferromagnetism) are also coupled. This coupling, known as magnetoelectric effect, gives place to extra degrees of freedom which may allow magnetization to be switched by an electric field and polarization to be switched by a magnetic field [2, 6, 7] (**figure 1.a**). Coexistence of ferroelectricity and ferromagnetism can, but need not lead to magnetoelectric coupling and actually only a subgroup of the multiferroic materials fulfills this condition (**figure 1.b**). In practice, magnetoelectric coupling can be achieved directly or indirectly via strain. In the first case, application of an electric field changes the local symmetry of the magnetic cations and, hence, changes their spin orientation. In the case of indirect coupling, change in local symmetry occurs due to the effects of strain. [2]. Indirect coupling gives rise to the preparation of composites with magnetoelectric coupling. As an example, the combination of a piezoelectric material intimately connected to a magnetoelastic material may lead to an indirect multiferroic behavior via strain.

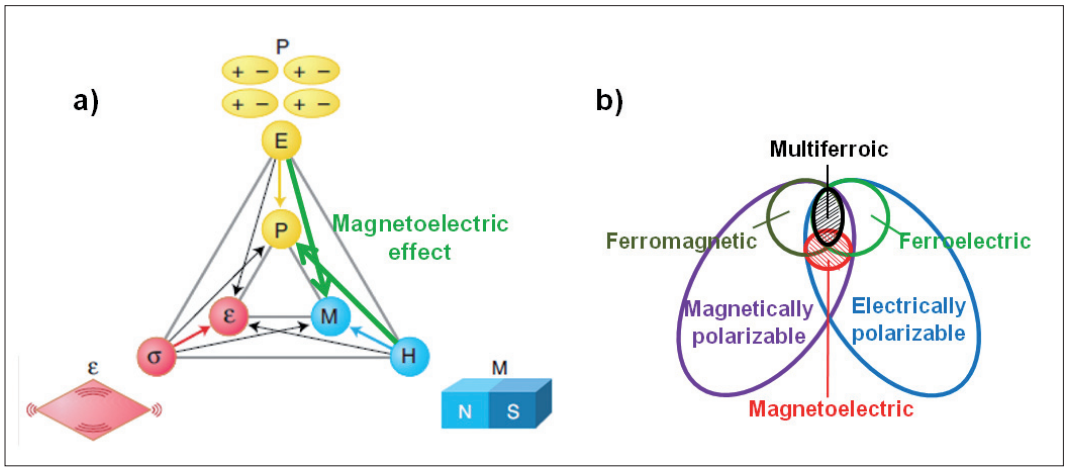

Figure 1. (**a**) Schematic representation of phase control in ferroics and multiferroics. The electric field (*E*), magnetic field (*H*), and stress (σ) control the electric polarization (*P*), magnetization (*M*), and strain (ε), respectively. In a magnetoelectric multiferroic, a magnetic field may control *P* or an electric field may control *M* which is represented by thicker arrows (adapted from [5]). (**b**) Relationship between ferroic, multiferroic and magnetoelectric materials (adapted from [2]).

Magnetoelectric materials can be used for typical applications of ferroelectric and ferromagnetic materials. However, their most potential applications are those derived from the possibility of switching magnetization under an electric field and vice versa. Thus, the extra degree of freedom provided by the magnetoelectric effect gives rise to new applications such as electromagnetic resonance devices controlled by electric fields, transductors with tunable piezoelectricity or, even most attractive, devices for memory storage [4, 8, 9]. Commercial magnetic memories use a magnetic field for writing information with two magnetic states (+M and –M) that represent magnetic bits "0" and "1". With the aim to protect the information the magnetic memories usually consist in hard magnetic materials that require a high coercive field. However this means high energy consumption and low writing speed. From this point of view it is currently considered that writing directly by an electric field may solve these shortcomings and, hence, this possibility, still in progress, have become the main driving force in multiferroic materials research.

Multiferroic materials can be divided into two general groups: single-phase multiferroics and composites or two-phase multiferroics. Single-phase multiferroics are those in which at least two "ferroic" properties are presented within the same phase. Instead, composites are multiphase systems in which each phase presents a different "ferroic" property. As previously mentioned, in composite multiferroics magnetoelectric coupling occurs indirectly via strain. According to their phase distribution there are different kinds of composite multiferroics and, actually, reports can be found in which an enhancement of several orders of magnitude in the magnetoelectring coupling respect to single-phase systems is described [2, 4]. However, a single-phase multiferroic with a strong coupling between its ferroelectric and its ferroelectric orders could allow an easier control of the magnetic nature through electric fields. Unfortunately, the number of known single-phase multiferroic materials is not very high.

The first material simultaneously showing ferroelectricity and ferromagnetism, the nickel iodine boracite $Ni_3B_7O_{13}I$, was discovered in 1966, [10]. That was followed by the synthesis of several multiferroic boracites, all of them with very complex structures and many atoms per unit cell. However, in spite of its incalculable value to proof the multiferroic concept, their practical applications are unavoidably hampered by their complex structures [11]. Subsequently the search for other magnetoelectrics began in Russia based on the idea of replacing the B cation of the perovskite-type ferroelectric phase for other cations with magnetic order. However, all these initial attempts again failed in obtaining a simultaneous ferroelectric and ferromagnetic with response within the same phase. It is not till the beginning of the 21st century when new improvements in understanding the phenomena implied in the simultaneous coexistence of magnetic and ferroelectric orders [11], together with novel synthesis methods and characterization techniques, have given rise to a renaissance in the field [5]. In year 2000 Nicola A. Hill [11] reported that the scarcity of multiferroic materials must be attributed to intrinsic factors since the requirements for symmetry and electric properties might be contradictory. From the point of view of symmetry there are 31 point groups that allow an electric polarization and 31 that allow a spontaneous magnetization, but only 13 point groups are found in both categories. However, the most exclusive requirements are those that deal with the electronic configuration. The presence

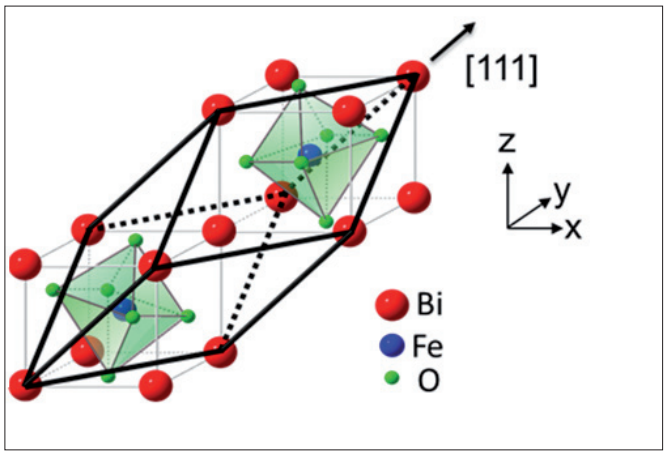

Figure 2 Schematic drawing of the crystal structure of perovskite $BiFeO_3$ (space group: *R*3c). Two crystals along [111] direction are shown in the figure. Adapted from [23].

Bol. Soc. Esp. Ceram. Vidr. Vol 53. 1, 1-14, Enero-Febrero 2014. ISSN 0366-3175. eISSN 2173-0431. doi: 10.3989/cyv.12014

of *d* electrons is necessary for the existence of a magnetic moment (and consequently for any kind of magnetic order), but at the same time the occupation of this *d* orbitals tends to reduce the crystallographic distortion which is necessary for ferroelectricity. For example in $PbTiO_3$ and $BaTiO_3$, both ferroelectric compounds showing a perovskite-type structure, the Ti^{4+} ions have a d^0 electron configuration. This electronic state facilitates the Ti 3d - O 2p hybridization which is essential for stabilizing the ferroelectric distortion [12]. On the other hand, the occupancy of the d-orbitals undergoes a Jahn-Teller distortion which, becoming the dominant effect, will decrease the centrosymmetric distortion required for ferroelectricity [11]. In other words, alternative mechanisms may explain the concurrent existence or ferroelectricity and magnetic order in magnetoelectric materials and, actually, reports can now be found which explore the possibilities of non-oxidic systems such as the $K_3Fe_5F_{15}$ or $Pb_5Cr_3F_{19}$ families [13, 14].

The case is that at present there are few known families of oxide materials that exhibit multiferroic behavior. The family of $REMn_2O_5$ manganites ($RE^{3+}Mn^{3+}Mn^{4+}O^{2-}_5$), where RE is a rare-earth ion from Pr^{3+} to Lu^{3+} (although it can also be Y^{3+} and Bi^{3+}) [15-17], is one of these systems displaying concurrent magnetic and ferroelectric order, although at temperatures below 30-40 K. Compounds belonging to this family have two low-temperature phase transitions. The nature of the first transition is not completely understood while the second one is simultaneously a magnetic and a ferroelectric phase transition [18]. In the particular case of the terbium manganite, $TbMn_2O_5$, it has been observed a highly reversible switching of the electrical polarization with moderate magnetic fields, ~ 0.2 T, which is very interesting for applications such as magnetically recorded ferroelectric memories. On the other hand the family of $REMnO_3$ ($RE^{3+}Mn^{3+}O^{2+}_3$) manganites can crystallize in the ortorrombic and the hexagonal symmetry (depending on the size of the RE^{3+} cation), but only those that show the hexagonal symmetry belonging to the spatial group P63cm exhibit ferroelectric order. This last group includes compounds where RE is Ho^{3+}, Er^{3+}, Tm^{3+}, Yb^{3+}, Lu^{3+} or Y^{3+}. Among them the yttrium manganite has been the most studied one; in that material the observed ferroelectricity is attributed to electrostatic and size effects, but not to changes related to chemical bounds (as in other perovskite-type ferroelectrics [15]).

Other group of materials with multiferroic behaviour are the perovskite oxides containing Bi^{3+} ($BiXO_3$ where X is a trivalent transition metal), as $BiMnO_3$ or $BiFeO_3$, in which the ferroelectricity arises from the stereochemical activity of the lone pair of electrons of bismuth atoms [11, 19]. More specifically bismuth ferrite ($BiFeO_3$) is one of the most promising multiferroic materials and the most studied in the last years. Its high phase transition temperatures ($T_{Néeel}$ = 370 ºC; T_{Curie} = 873 ºC) explains the high interest in this material which, actually, is one of the few known materials that can be used as multiferroic at room temperature. The compound $BiFeO_3$ was synthesized for first time at the late fifties. The physical and structural properties of $BiFeO_3$ were source of controversy during the 60´s and 70´s, although since the early 60´s the first signals about $BiFeO_3$ being simultaneously antiferromagnetic and ferroelectric were already observed. Actually the ferroelectric nature of $BiFeO_3$ remained uncertain until 1970, when ferroelectric measurements in $BiFeO_3$ single crystals showed a spontaneous polarization of 6.1 $\mu C/cm^2$. Later in 2003, the discovery of a room temperature spontaneous electric polarization unusually high (~ 50-60 $\mu C/cm^2$) in $BiFeO_3$ thin films [20], promoted a renewed interesting in this material which continues nowadays. Furthermore, ab-initio calculations even suggest spontaneous polarization values of about 90-100 $\mu C/cm^2$ [21], something which is consistent with that work of Wang et al. in 2003 [20].

2. $BiFeO_3$ STRUCTURE

At room temperature and atmospheric pressure, $BiFeO_3$ shows a rhombohedrically distorted perovskite structure belonging to the special group R3c (α-$BiFeO_3$ phase). Unit cell parameters are a_{rh} = 3.965 Å and α_{rh} = 89.3-89.4°. The $BiFeO_3$ unit cell can be also described in the hexagonal symetry where $a_{hex}=b_{hex}$=5.58 Å and c_{hex}=13.90 Å [22]. Another important structural parameter is the rotation angle of the oxygen octahedral, related with the Goldschmid tolerance factor for perovskites (*t*). For $BiFeO_3$ *t* tolerance factor is 0.88 so the oxygen octaedra must buckle in order to fit into a too small cell [22] resulting in a Fe-O-Fe angle (θ) value of 154-156º [22].

In some particular cases certain discrepancies have been found regarding the crystal structure of α-$BiFeO_3$ at room temperature. As an example, in crystals with a lower grain size than 30 nm it has been observed a progressive change from rhombohedric to cubic symmetry [24]. In the case of epitaxial $BiFeO_3$ films different structures have been suggested such as rhombohedral, tetragonal and monoclinic [20, 25]. Recently, it has also been proposed that the space group P1 could be more appropriated than the well accepted polar space group R3c to describe the structure of α-$BiFeO_3$ at room temperature [26].

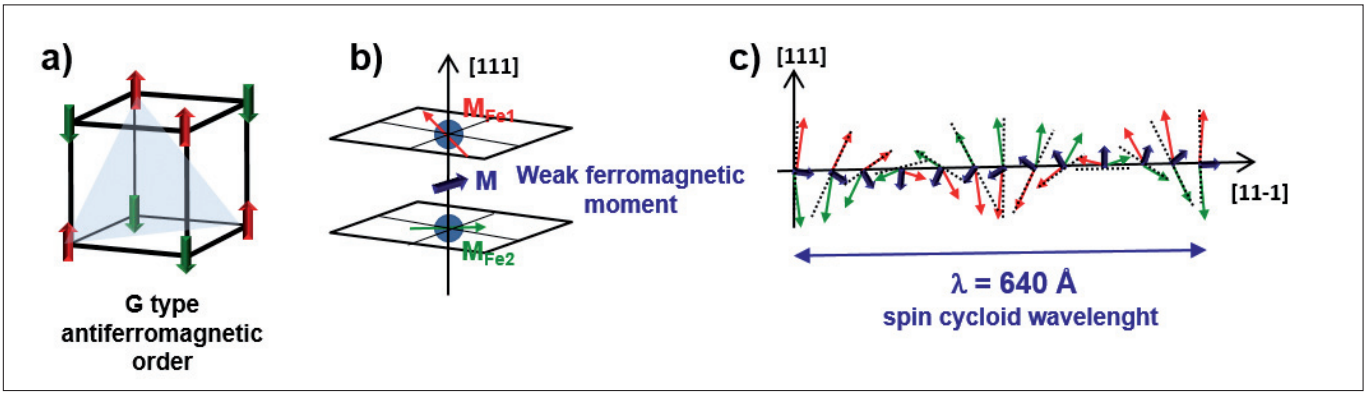

Figure 3. $BiFeO_3$ magnetic structure showing the origin of the G-type antiferromagnetic order (adapted from [1]) (**a**), the formation of the weak magnetic moment (adapted from [1]) (**b**) and the spin cycloid superstructure (adapted from [29] (**c**).

Ferroelectricity in $BiFeO_3$ is originated by the stereochemically active lone-pair orbital of bismuth ions ($6s^2$), which being largely displaced with regards to the FeO_6 octahedra, generates a spontaneous polarization along the [111] axis of the rhombohedral unit cell [1, 27]. On the other hand, $BiFeO_3$ is a G-type anti-ferromagnet [22, 28] (**figure 3.a**) in which all neighboring magnetic spins are oriented antipararell to each other. As a consequence of the oxygen octahedral distortion, directly related with the Fe-O-Fe angle, $BiFeO_3$ structure presents spin canting which results in a weak magnetic moment in the unit cell according with Dzyaloshinskii-Moriya interaction [1, 29] (**figure 3.b**). However, this net magnetic moment exhibits a long-range superstructure consisting on a spin cycloid with a 64-nm wavelength (**figure 3.c**) that is incommensurable with the crystallographic structure [29, 30]. The result is that, for single-crystals with size fairly larger than the spin cycloid, the net magnetization is zero which, at first, prevents a magnetoelectric effect. The magnetoelectric effect may be recovered by frustration of the spin cycloid. As it will be described later, this can be achieved by different methods.

At temperatures around 370 ºC a second order phase transition is produced which has been assigned to the transition from anti-ferromagnetic to paramagnetic structure of $BiFeO_3$ [22, 31, 32]. This magnetic transition is associated with anomalous lattice expansion [32]. Around 825 ºC a first order transition is produced from the paramagnetic α-$BiFeO_3$ phase to the high temperature phase β-$BiFeO_3$ [33]. This first order transition is accompanied by an abrupt decrease of the unit cell volume [32, 34, 35] as well as abrupt changes in atomic positions [32]. Besides, this transition is also accompanied by a maximum in the dielectric constant assigned to the transition from ferroelectric to paraelectric [34]. On the other hand, the symmetry of the β-$BiFeO_3$ phase has been subject of much controversy in literature. Nevertheless, most of authors agree that it is centrosymmetric [22, 32, 35-37] corroborating that the phase transition at 825 ºC is the ferroelectric to paraelectric transition. In 2008, Hamount et al. [36] reported that β-$BiFeO_3$ shows a monoclinic symmetry belonging to the spatial group P21/m with a monoclinic angle value of 90.01°. However, Palai et al. [35] proposed that β phase is orthorhombic, although with some coexistence of rhombohedral domains. In any case these authors were unable to establish the spatial group of this phase from their experimental data. On the other hand, in the same year Selbach et al. [32] suggested that β phase is rhombohedral, belonging to the spatial group R(-3) c. This assertion is not accepted by other authors which state that the transition at 825 ºC could not be ferroelastic (as it is inferred from the changes in the ferroelastic domains configuration) if the symmetry of both the α and the β phases is rhombohedral [22, 35]. The reasons for these contradictions can be found on the difficulty for obtaining a pure $BiFeO_3$ phase and the complexity associated with sample characterization. On one hand, the presence of secondary phases complicates the structural characterization of the paraelectric phase [32, 35]. On the other hand, X-Ray diffraction technique has a poor sensitivity to the positions of the oxygen atoms as a consequence of their low electronic density compared with that of bismuth or iron atoms [22]. In this sense, high temperature neutron diffraction is a much more illustrating technique. So, based on this last characterization technique, Arnold et al. [37] asserted that β-phase symmetry is orthorrombic although with some phase coexistence, as had been proposed earlier [35]. In fact, in 2010 Selbach et al. [38] rectified their first proposal of a rhombohedral symmetry [32] to accept the orthorrombic symmetry proposed by Arnold et al. [37].

At higher temperature, around 933 ºC, a second order phase transition from β to γ phase of $BiFeO_3$ has been reported to occur [35], although this transition is not considered intrinsic by some other authors [33]. For this high temperature phase a cubic symmetry belonging to the space group Pm(-3) m has been suggested [35]. Besides, it has been observed that the transition from the β phase with orthorhombic symmetry to the γ phase with cubic symmetry is accompanied with a sharp decrease of the band-gap towards zero, indicating that at this temperature the transition from an electric insulator to a metallic behavior is produced [35].

3. EQUILIBRIUM PHASES IN THE Bi_2O_3-Fe_2O_3 SYSTEM

The first phase diagrams for the Bi_2O_3-Fe_2O_3 system were published in the mid-60´s [39]. Years later, modifications to these initial diagrams were published [33, 35, 36, 40, 41] (**figure 4**), although with certain discrepancies between them. For example, in some diagrams [33, 40, 41] the α-Bi_2O_3 → γ-Bi_2O_3 phase transition is also extended to the compatibility region between $Bi_{25}FeO_{39}$ (or $Bi_{25}FeO_{40}$) and $BiFeO_3$ phases, which is considered by other authors [35] as an indication of a non equilibrium state. In the same way, subtle differences can be found on the temperature at which a liquid phase first appears (from 745 ºC [40] to 792 ºC [41]), on the temperature at which the $Bi_2Fe_4O_9$ decomposes (from 934 ºC [41] to 961 ºC [35]), as well as on the temperature for the $BiFeO_3$ peritectic decomposition (from 852 ºC [33] to 934 ºC [41]), this latter more noticeable. Moreover, according to Palai et al. [35] the peritectic decomposition of $BiFeO_3$ occurs from the γ phase, but this phase is not considered as thermodynamically stable by other authors [33]. Attempts to explain these discrepancies attribute them to an uncontrolled level of impurities and to

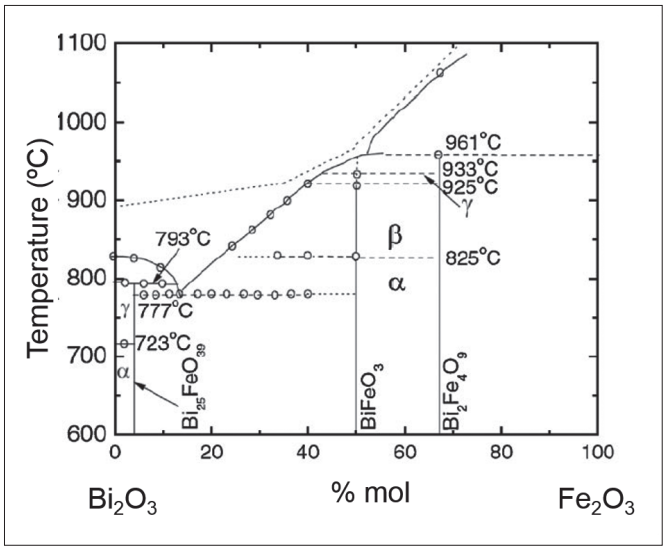

Figure 4 Compositional phase diagram of the Bi_2O_3-Fe_2O_3 system proposed by Palai et al. [35] (adapted from [35]).

Bol. Soc. Esp. Ceram. Vidr. Vol 53. 1, 1-14, Enero-Febrero 2014. ISSN 0366-3175. eISSN 2173-0431. doi: 10.3989/cyv.12014

the presence of defects in the as-prepared samples [33], but also to data being collected under non-equilibrium conditions [35]. Although in the phase diagrams there is one point of agreement, the $BiFeO_3$ phase being thermodynamically stable in a wide range of temperatures, the case is that controversy remains open and contradictory data that question both the diagram and the stability itself of the $BiFeO_3$ phase are currently being published.

Actually many works in the specialized literature claim the difficulty in obtaining a pure $BiFeO_3$ phase and the unfeasibility to avoid the presence of secondary phases [40, 42-45]. According to the phase diagrams, slight deviations from the stoichiometric composition would result in a mixture of $BiFeO_3$ and $Bi_{25}FeO_{40}$ phases if we move to Bi_2O_3 rich compositions or in a mixture of $BiFeO_3$ and $Bi_2Fe_4O_9$ if we move to the Fe_2O_3 rich area, but it would be possible to obtain a pure $BiFeO_3$ with a careful stoichiometric control. Furthermore, the coexistence of the three phases in an equilibrium state has been as well reported [43], although according to the Gibbs phase rule this situation is in fact incompatible for a binary system. Based on this idea Valant et al. [43] suggested that in the presence of tiny amounts of impurities, the Bi_2O_3-Fe_2O_3 system behaves as a pseudo-binary system: slight deviations from the nominal composition will considerably increase the proportion of secondary phases, particularly if impurities are incorporated into the $Bi_{25}FeO_{39}$ bismuth-rich phase (the corresponding phase field in the phase diagram would significantly narrow).

On the other hand, some other authors assert that bismuth ferrite is actually a metastable phase [44, 45], so under certain conditions it will decompose to yield the secondary $Bi_2Fe_4O_9$ and $Bi_{25}FeO_{39}$ phases according to **reaction 1:**

$$49\ BiFeO_3 \rightarrow 12\ Bi_2Fe_4O_9 + Bi_{25}FeO_{39} \quad [1]$$

Again, the conditions at which $BiFeO_3$ decomposes are source of discussion. For example Morozov et al. [40] stated that $BiFeO_3$ decompose at temperatures higher than 780 ºC. On the contrary, Carvalho et al. [44] avowed that $BiFeO_3$ decomposes at temperatures below 600 ºC, being possible to obtain a pure phase with a fast cooling that avoids its decomposition. In 2009, by means on high temperature X-ray diffraction measurements Selbach et al. [45] asserted that $BiFeO_3$ is metastable from 447 up to 767 ºC. In this range of temperatures the $Bi_2Fe_4O_9$ and $Bi_{25}FeO_{39}$ secondary phases would have a slighly higher stability than $BiFeO_3$. Thus, the pure $BiFeO_3$ phase could be obtained at temperatures slighly higher than 767 ºC, with a fast heating to avoid the initial formation of $Bi_2Fe_4O_9$ and $Bi_{25}FeO_{39}$ phases and a fast cooling to avoid the decomposition of the $BiFeO_3$ reacted phase. Due to the small Gibbs energy difference between the $BiFeO_3$ and the decomposition products ($Bi_2Fe_4O_9$ and $Bi_{25}FeO_{39}$) minor variations may shift the equilibrium of the $BiFeO_3$ formation/decomposition reactions (**reaction 2**):

$$12\ Bi_2Fe_4O_9 + Bi_{25}FeO_{39} \leftrightarrows 49\ BiFeO_3 \quad [2]$$

For example, in consonance with the proposal by Valant et al. [43] the presence of impurities with a larger solubitily in the $Bi_2Fe_4O_9$ or $Bi_{25}FeO_{39}$ secondary phases than in the $BiFeO_3$ may increase the stability range of these secondary phases shifting the equilibrium of **reaction 2** towards the left.

4. SYNTHESIS OF SINGLE-PHASE $BiFeO_3$

4.1. Mixed oxides synthesis

$BiFeO_3$ compound was for the first time synthesized in Russia by the mid 50´s, using the conventional mixed oxides synthesis method [46]. Around that time, different authors reported that $BiFeO_3$ could be synthesized by the solid state reaction of Bi_2O_3 and Fe_2O_3 precursors at temperatures around 700 and 800 ºC with annealing times from 30 to 120 min. However, in 1967 Achenbach et al. [42] pointed out the difficulty of obtaining a pure $BiFeO_3$ phase. According to these authors all attempts to obtain pure $BiFeO_3$ result in multiphase products in which $BiFeO_3$ comes together with small amounts of parasite phases. Furthermore, modifications in the temperature, time or atmosphere of the annealing treatment, repeated firing and grinding or even the addition of small amounts (< 0.5 mol %) of a third component did not ever lead to a pure $BiFeO_3$ phase. These authors also reported that at temperatures below 700 ºC the formation reaction of $BiFeO_3$ is incomplete, at temperatures between 700 and 750 ºC $BiFeO_3$ formation competes with the $Bi_2Fe_4O_9$ secondary phase formation and, finally, at temperatures above 750 ºC $BiFeO_3$ becomes unstable and decomposes. In view of these impediments Achenbach et al. suggested a method to obtain a pure $BiFeO_3$ phase without secondary phases which is still used nowadays by many research groups [26, 47]. This method lies in shifting the nominal composition towards a composition with a certain Bi_2O_3 excess. According to the phase diagrams, firing such composition at temperatures around 750 ºC leads to a mixture of $BiFeO_3$ plus unreacted Bi_2O_3. Finally this Bi_2O_3 excess can be lixiviated by leaching with concentrated HNO_3, resulting in a pure $BiFeO_3$ phase to the X-ray diffraction characterization.

In 2003 Morozov et al. [40] asserted that the solid-state synthesis of a pure $BiFeO_3$ is not viable due to the fact that its decomposition temperature is lower than its activation one. Not much later Wang et al. [48] suggested a new method to obtain a pure $BiFeO_3$ phase. This method, so-called "rapid liquid phase sintering", consists in the thermal treatment of the oxide precursors at high temperatures (880 ºC) during a brief period of time (450 s) and applying extremely fast heating and cooling rates (100 ºC/s). These authors claim that the presence of a liquid phase (the thermal treatment takes place at temperatures above the melting point of Bi_2O_3), together with the fast heating rate, efficiently accelerate the formation reaction of $BiFeO_3$ phase and prevent the secondary phase formation. Following Wang et al.'s publication this rapid liquid phase sintering method has been frequently employed by different authors to synthesize $BiFeO_3$ apparently free of secondary phases [49, 50]. For example Pradhan et al. [49] have studied the effect of slight variations in the annealing conditions concluding that the temperature must be exactly 880 ºC in order to obtain a pure phase; lower temperatures (850 ºC) lead to an incomplete reaction, whereas higher temperatures (slightly higher: 890 ºC) render multiphase products as a consequence of the Bi_2O_3 volatilization. On the other hand Yuan et al. [50] analyzed the influence of the particle size of the precursor powders. These authors realized that working with Bi_2O_3 or Fe_2O_3 of an average particle size > 1 μm impedes the formation reaction to be completed and again results in a final product with small amounts of secondary phases.

However the obtaining of a pure $BiFeO_3$ phase by the rapid liquid phase sintering method of Wang and co-workers was later questioned by other authors, mostly because on those works the presumption of a pure $BiFeO_3$ phase is just based on a rough characterization just by means of X-ray diffraction (a technique that actually shows low sensibility to phases composed by relatively lighter elements, like the iron rich $Bi_2Fe_4O_9$ phase). In particular in 2007 Valant et al. [43] evidenced that the conventional solid-state process may lead to a $BiFeO_3$ phase in the XRD patterns as pure as that obtained through the liquid phase sintering method. However, when going to the scanning microscope appreciable amounts of secondary phases are easily detectable in both cases. Actually this lack of rigorous characterization is still found in many current works reporting a pure $BiFeO_3$ phase, probably explaining the mentioned discrepancies. But besides, the work of Valant and co-workers also suggested that, since the coexistence of three phases in equilibrium is incompatible with a binary system (Bi_2O_3-Fe_2O_3), the secondary phases are stabilized by trace levels of impurities whose presence cannot be easily controllable during the synthesis process. Only by using extremely pure reagents (≥ 99.9995 %) a pure $BiFeO_3$ phase was attained by these authors after annealing at 800 ºC during 5 hours. In any case, although the effect of impurities is certainly accepted, some groups still stand up for the metastability of the $BiFeO_3$ phase [35, 45, 51].

But, as mentioned before, another strategy that has been exploited in order to facilitate the synthesis of $BiFeO_3$ by a mixed-oxides route entails the addition of small amounts of a third component. These additives could substitute the Bi^{3+} or Fe^{3+} cations at the A or B positions of the perovskite structure and, hence, can contribute to stabilize the $BiFeO_3$ with respect to the secondary phases. And, what is more, the addition of external dopants may as well be helpful to improve the magnetoelectric properties of the synthesized product. Thus, it has been described in the literature that rare earth dopants like La^{3+} [52, 53], Gd^{3+} [52, 54], Nd^{3+} [52], Sm^{3+} [52, 55], Y^{3+} [56], or Ho^{3+} [57] may have the desired effect of stabilizing the $BiFeO_3$ phase and decreasing the amount of secondary phases when replacing some Bi^{3+} cations in the A positions of the perovskite structure. However, these dopants may diminish the electric polarizability of the A positions [52, 58, 59], so alternatively the use of transition ions like Mn^{3+} [60] or Ti^{4+} [61-63] for substituting the Fe^{3+} cations in B positions, has been recently proposed. Nevertheless, the addition of a third component must be taken cautiously since in many cases they can have the contrary effect stabilizing one of the secondary phases (or both of them) [63-66], with an analogous result to that described by Valant et al. [43].

4.2. Synthesis by chemical routes

In order to get a pure $BiFeO_3$ avoiding byproducts of secondary phases, chemical synthesis routes have been widely used. One of them is co-precipitation synthesis [67-72] which lies in the simultaneous precipitation of different elements at certain pH and concentration conditions. A subsequent thermal annealing leads to the chemical reaction between the co-precipitated hydroxides to get the final complex oxide. Co-precipitation synthesis represent two main advantages with regards to the mixed-oxides method: a lower contamination probability and a higher reactivity [73]. Therefore, this method improves the reaction kinetics minimizing impurities that could stabilize the secondary phases.

Several authors assert that it is possible to obtain a pure $BiFeO_3$ by a co-precipitation synthesis method [67, 68, 70, 71]. However, the precise conditions to avoid the formation of secondary phases are in some cases contradictory. For example, whereas Ke et al. [68] uphold that a bismuth excess is required to compensate volatilization during annealing, both Liu et al. [70] and Chen et al. [67] argue that it is possible to obtain a pure $BiFeO_3$ by starting from the stoichiometric composition. On the other hand, according to Shami et al. [71] a pure $BiFeO_3$ single phase will be obtained by co-precipitation route if Bi_2O_3 is used as the Bi^{3+} precursor instead of the generally used $Bi(NO_3)_3 \cdot 5H_2O$. However, once again most of these publications lack of an accurate characterization (merely XRD) so any conclusion must be observed cautiously.

Besides co-precipitation, other chemical routes such as sol-gel, the Pechini method or the like have as well been considered in order to prepare a pure $BiFeO_3$ phase. In some cases these methods seem successful in order to obtain $BiFeO_3$ nanoparticles [74-78], but divergences are also frequent. Actually it has been suggested that the $BiFeO_3$ obtained by these wet chemistry routes evidences a metastable behavior and under certain conditions - again contradictory [44, 68]- it decomposes leading to secondary phase byproducts.

Another chemical strategy which has been recently studied to synthesize the $BiFeO_3$ pure phase is the hydrothermal (or solvothermal) processing. Actually during the past decades hydrothermal processing has become a very attractive method for the synthesis of advanced materials due to its intrinsic benefits like a high compositional and morphological control as well as a high purity of the obtained powders by avoiding subsequent annealings or milling treatments [79]. Accordingly, in 2006 Han et al. [80] and Chen et al. [81] reported the obtaining of micron-sized particles of pure $BiFeO_3$ by applying a hydrothermal route. However, once again the lack of a thorough characterization of the obtained products questions the inexistence of secondary phases. The case is that slight variations in the temperature, pressure and/or pH parameters resulted in the formation of secondary phases and, even, in obtaining only some other phases of the Bi_2O_3-Fe_2O_3 system, such as $Bi_{12}Fe_{0.63}O_{18.945}$ or $Bi_2Fe_4O_9$ [80]. In 2007 Wang et al. [82] achieved the synthesis of spherical $BiFeO_3$ nanoparticles by addition of a small amount of KNO_3. According to these authors small changes in the experimental conditions can also lead to the formation of different phases. For example, when using $LiNO_3$ instead of KNO_3 as mineralizer a pure $Bi_{25}FeO_{39}$ phase is obtained [83]. However, it has been also reported that using potassium salts as precursors may result in $BiFeO_3$ crystals that contain K^+ cations incorporated into the perovskite structure [84]. But after these early works, the current research regarding the hydrothermal synthesis $BiFeO_3$ is mainly focused on understanding the mechanisms implied in the hydrothermal reaction [85], the effect of systematic variations in the experimental conditions [86, 87], the effect of quelants or surfactants [88-91], the crystal growth mechanisms [87, 90] and/or the obtaining of $BiFeO_3$ particles with tailored morphology [87, 90].

Furthermore, it has also been reported that the microwave-assisted hydrothermal approach gives a considerable

improvement in crystallinity and purity of the obtained $BiFeO_3$ samples with respect to the traditional hydrothermal processes [92-94]. However, the specific conditions in which a pure $BiFeO_3$ phase is obtained are again contradictory among different works. Some authors report that the use of the adequate mineralizer (either KOH [92] or NaOH [94]) under a short reaction time lead to a pure $BiFeO_3$ phase according to the XRD characterization whereas others defend that a N_2 or a H_2 atmosphere is required in order to obtain pure $BiFeO_3$ ceramics by this method [95].

4.3. Mechanochemical synthesis

One additional method currently used for preparing pure $BiFeO_3$ powders is the mechanochemical synthesis. This method allows the obtaining of different complex oxides within one step, also avoiding subsequent thermal annealing. In many cases, products obtained by this method are nanoparticles with a high sinterability. However, the main advantage of this method is the possibility to obtain metastable phases which are tricky to obtain by other conventional synthesis methods [96].

In 2007 Szafraniak et al. [97] reported the synthesis of $BiFeO_3$ particles by a mechanochemical route at room temperature. The obtained product consists of irregular agglomerates of nanoparticles of ~50 nm in size. HRTEM characterization shows that nanoparticles present a core-shell structure with crystalline $BiFeO_3$ as a core and an amorphous shell of 1-2 nm thick. Similar results have been more recently obtained by Da Silva et al. [98]. These authors have proven the high reactivity of the amorphous shell, concluding that these areas play a key role in the mechanically induced chemical reactions. Besides, the mechanochemical synthesis of $BiFeO_3$ doped in A positions with different ions such as Eu^{3+} [99], Sm^{3+} [100], Sr^{2+} [101]; of $BiFeO_3$ co-doped in A and B positions with Ba^{2+} and Mn^{2+} respectively [102]; as well as of complex systems comprising $BiFeO_3$ and other perovskite structures such as $PbTiO_3$ [103] or $BaTiO_3$ [104] has also been studied.

5. FABRICATION OF DENSE $BiFeO_3$ BULK MATERIALS

Sintering is the consolidation step of the ceramic material during which energy is provide to the system in order to activate different physical and chemical processes that lead to particle joining and porosity releasing. Sintering also drastically changes the functional microstructure of the ceramic material which, in fact, is closely related to its properties [73, 105]. Densification of bismuth ferrite is tricky and materials with a density not higher than 90 % of the $BiFeO_3$ theoretical density are usually obtained. The high porosity content in $BiFeO_3$ materials is a severe impediment for most practical applications. During sintering, both grain growth and densification occur simultaneously. Thus, equilibrium between these two processes – that are usually competitive – will have a key influence on the microstructure of the final material [73]. Generally speaking, it is necessary to find a sintering temperature and time regime in which the mechanisms involved in densification prevail over those involved in grain coarsening. In the particular case of $BiFeO_3$ materials, these problems with densification must be added to the above mentioned synthesis complexity and thermal stability of this compound, so making the sintering step even more critical.

As mentioned, rapid liquid phase sintering is a method frequently used to obtain $BiFeO_3$ materials [48-50, 106]. In the Bi_2O_3-Fe_2O_3 system, annealing at temperatures above ~ 775 ºC may result in the formation of a Bi-rich liquid phase [35]. So, at these conditions, sintering will be influenced or even controlled by the presence of the liquid phase. If this liquid suitably wets and covers the surface of the solid particles then it may provide a high diffusivity path to matter transport [105]. In order to create a liquid phase during the sintering of $BiFeO_3$ materials, the stoichiometry must be slightly enriched in bismuth; alternatively, the material may have compositional heterogeneities with Bi-rich areas. Typically when using this sintering method the liquid phase formation is achieved by conducting both the synthesis and the sintering processes in one single step, taking the reactants to high temperatures at a rapid heating rate [48]. Even though, the obtained density values are still not higher than 92 % of the $BiFeO_3$ theoretical density [48, 50]. Besides, due to the presence of the liquid phase an undesired exaggerated grain growth may not be avoided when using this method [49]. As an example, micrographs of materials obtained by this method are shown in **figure 5**.

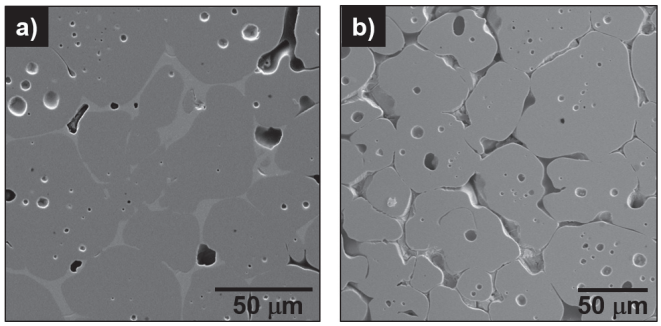

Figure 5. Scanning electron micrographs of $BiFeO_3$ ceramics (polished (**a**) and chemically etched (**b**) surfaces) sintered at 850 ºC in presence of a Bi-rich liquid phase that lead to an exaggerated grain growth.

Furthermore, the high temperature during sintering may also result in a loss of stoichiometry as a consequence of bismuth volatilization. These problems are usually avoided by using a Bi-excess in the nominal composition [68] as well as by covering the sample with powders of the same composition and running the thermal treatment in a closed crucible [107, 108].

Recently the use of spark-plasma sintering (SPS) has been tested as an alternative way to improve the densification in $BiFeO_3$ bulk materials [47, 109, 110]. This sintering method is quite useful to promote the densification mechanisms without leading crystal growth [109, 111]. Density values around 96 % of the theoretical density have already been reported for $BiFeO_3$ ceramics prepared by SPS [47, 109]. However, although in some of the published works a pure $BiFeO_3$ phase is detected by X-ray diffraction [109], the corresponding SEM micrographs do show rests of liquid phase that suggest the presence of secondary phases.

5.1. Defect chemistry in $BiFeO_3$ materials

For a complex oxide like $BiFeO_3$ the punctual defects that must be considered are the creation of cationic or anionic vacancies, the stoichiometric deviations and the changes in the oxidation states of Fe^{3+} or Bi^{3+} cations.

At first instance, the possible volatilization of Bi_2O_3 during the thermal treatment may result in a loss of stoichiometry, giving rise to the formation of either Fe-rich phases or the appearance of bismuth and oxygen vacancies ($V_{Bi}^{'''}$ and $V_O^{\cdot\cdot}$, respectively) in the $BiFeO_3$ structure. This can be expressed in terms of the Kröger-Vink notation according to **reaction 3**:

$$2\ Bi_{Bi} + 3\ O_O \rightarrow 2\ V_{Bi}^{'''} + 3\ V_O^{\cdot\cdot} + Bi_2O_3 \uparrow \quad [3]$$

Besides, the presence of bismuth vacancies may result in the occupation of the empty A sites by iron cations, leading to non-stoichiometric samples with $(Bi_{1-x}Fe_x)FeO_3$ composition as proposed by Morozov et al. [40]. In addition to this, it has been also proposed that as a consequence of the thermal treatment Fe^{3+} cations may reduce its oxidation state from III to II [48]. This would result in Fe^{2+} ions at the B-sites of the perovskite structure and will lead to oxygen vacancies in order to reach the charge neutrality (**reaction 4)**:

$$Fe_{Fe}^{\ x} \rightarrow Fe_{Fe}^{'} + 1/2\ V_O^{\cdot\cdot} \quad [4]$$

The presence of Fe^{2+} ions in $BiFeO_3$ materials has been widely studied [47, 93, 95, 112-115] considering that it may have a key role in the electromagnetic properties. In this sense, although analyses on $BiFeO_3$ single crystals by X-ray photoemission spectroscopy (XPS) has just detected iron in the 3+ oxidation state [112], more recent studies through Mössbauer spectroscopy [93] point towards the presence of a small amount of Fe^{2+} in low spin configuration in $BiFeO_3$ ceramic powders. Actually the fluctuations in the oxidation state of iron cations can be promoted by applying a gas flux (air, O_2, N_2 or Ar) during the thermal treatment [47, 95, 115]. For example, Kumar et al. [115] reported that an Ar flux during processing $BiFeO_3$ ceramics by a sol-gel method can modify the Fe^{3+}/Fe^{2+} ratio as well as the proportion of secondary phases (their amount seems to decrease when compared to ceramics obtained under an air flux).

5.2. Obtaining of doped $BiFeO_3$ bulk materials

The addition of dopants to $BiFeO_3$ materials (with the aim of stabilize the perovskite phase and/or modify its properties) can have a noticeable effect in both the densification and microstructural development during sintering.

As described in the literature the grain growth during sintering can be inhibited through the addition of dopants as La^{3+} [108], Sm^{3+} [116], Zn^{2+} [65], Pb^{2+} [117], Nb^{5+} [63, 118] or Ti^{4+} [61, 62]. Grain growth control by the effect of a third component is in fact very common in polycrystalline ceramics. In general, there are two mechanisms by which grain growth could be inhibited: the pinning and the solute drag effects. The pinning effect is produced when small particles of a secondary phase are pinned onto the grain boundaries, thereby restricting the diffusion processes that cause grain growth. On the other hand, the solute-drag effect is produced when the dopant (also called solute) is segregated to the grain boundaries due to a low solubility on the host component. Located at the grain boundaries, this solute slows down the diffusion resulting in an inhibition of grain growth [73] (**figure 6**). On the other hand when doping with aliovalent cations -those showing a different oxidation state that the cation to substitute- defects will be formed in order to neutralize the charge excess

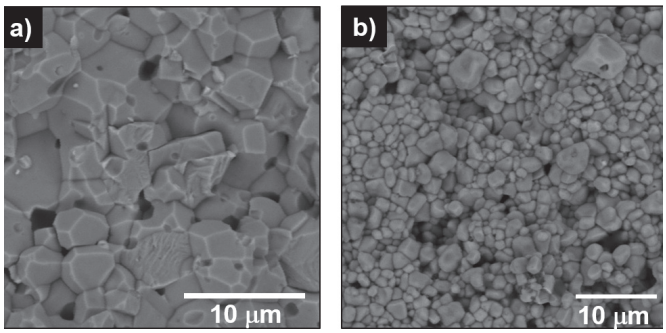

Figure 6. Scanning electron micrographs of the fracture surface of undoped (a) and Zn-doped (b) $BiFeO_3$ ceramics prepared by a mixed oxide route in similar conditions (800 ^oC during 2 h).

introduced by the dopant. In the case of acceptor dopants, the substitution will introduce an excess of negative charge. This can be compensated by different defect reactions, like creation of oxygen vacancies [119] or oxidation of pre-existing Fe^{2+} ions to Fe^{3+} [117]. In contrast, in case of donor dopants, the substitution will introduce an excess of positive charge. This charge can be compensated through reduction of Fe^{3+} to Fe^{2+} [114, 120], annihilation of oxygen vacancies [121] or creation of Bi^{3+} or Fe^{3+}cationic vacancies [122]. These defects may also affect the grain growth [61, 62].

6. PREPARATION OF $BiFeO_3$ THIN FILMS

From the point of view of microelectronics applications, the obtaining of materials in the shape of thin films is a key point. Typically the layer thickness must lie from a few fractions of nanometers up to cents of nanometers. As a result the material will have a strong interaction with the substrate, implying great changes in processing and properties compared with bulk materials. For example, as previously explained, the crystalline structure of bismuth ferrite can shift from rhombohedral to orthorrombic in epitaxial $BiFeO_3$ thin films [20]. Besides, such interaction with the substrate may also originate preferential orientation, stress or texturation.

In order to obtain $BiFeO_3$ thin films, different deposition methods have been employed. Among those based on physical evaporation techniques, pulsed laser deposition (PLD) and sputtering are the most used. In these techniques, atoms are ejected from a solid target material due to bombardment with energetic ions that are obtained from plume plasma which is generated in the sputtering chamber after applying an rf alternating current, a magnetic field or a laser beam. During the deposition the different experimental parameters – atmosphere and pressure of deposition, time of deposition or target composition – must be controlled. In this sense several works that study the optimal conditions for obtaining highly crystalline $BiFeO_3$ thin films using these methods [123-125] can be found in the literature. However, the problems related with the presence of secondary phases and heterogeneities seem to be persistent. For example Ternon et al. [123] were unable to obtain films which were free of parasitic phases and showed a dense and homogeneous microstructure at the same time. Lee et al. [124] studied the effect of deposition time in the crystallization and properties of films deposited on $Pt/Ti/SiO_2/Si(100)$ substrates. These authors observed that the increase in thickness after long deposition times was

accompanied by a decrease in the relative amount of Bi_2O_3 secondary phase (which was only observed at the interface with the substrate). Qui et al. [125] studied the differences between applying high temperatures during the deposition stage or applying a subsequent thermal annealing. According to these authors the microstructure displays a higher density in the first case, although the deposited layer does not present suitable ferroelectric properties. The influence of substrates in thin films prepared by sputtering has also been studied concluding that substrates like $SrRuO_3$ [126, 127] or $LaNiO_3$ [128] favor the $BiFeO_3$ crystallization.

With regards to the chemical deposition methods, the most common are chemical solution deposition (CSD), chemical vapor deposition (CVD), metal organic chemical vapor deposition (MOCVD), spin-coating and sol-gel. In order to obtain high quality layers by these chemical deposition methods the parameters of the deposited solution as well as the thermal annealing conditions must be controlled. For example, by carefully controlling these variables Das et al. [129] successfully prepared transparent $BiFeO_3$ films by spin-coating over glass substrates. Besides, reports can also be found in which the preparation of single-phase $BiFeO_3$ thin films is obtained through doping strategies [130, 131]. Nevertheless, in most of these works an insufficient characterization of the structure and microstructure of the films is still provided.

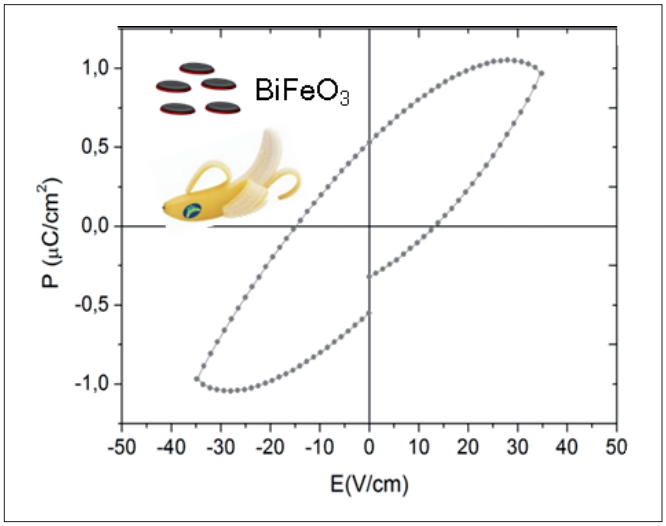

Figure 7. Measurement of the polarization vs. applied field for a $BiFeO_3$ bulk ceramics prepared by mixed oxide method. The obtained loop is similar to those generally reported in literature for $BiFeO_3$ ceramics and is also similar and those obtained when measured some foodstuff, for example the skin of a banana Adapted from Scott [133].

7. ELECTROMAGNETIC PROPERTIES IN $BiFeO_3$ MATERIALS

7.1. Electric response in $BiFeO_3$ materials

One of the most important shortcomings of $BiFeO_3$ materials regarding its possible practical applications is the high electrical conductivity that they usually present [22]. This high electrical conductivity makes impossible the polarization of the materials and, hence, hampers its use as ferroelectrics.

The ferroelectric cycles commonly described in the literature for $BiFeO_3$ materials usually indicate a high remnant polarization (Pr), although they habitually display a worrisome rounded shape [48, 49, 132] (**figure 7**). One example of this kind of cycles would be those published by Wang et al. [48] in a work asserting an enhancement of the polarization which has been cited more than 400 times since it was published in 2004. However, later in 2008, Scott [133] compared the cycles usually reported for $BiFeO_3$ materials with those obtained for domestic objects or even for some foodstuff, like for example the skin of an Ag-electroded banana. As Scott demonstrated, the fact is that this kind of cycles is characteristic of materials with a high electrical conductivity so they have little to do with the ferroelectric properties of the material.

Actually a general agreement on the reasons for the high electrical losses in $BiFeO_3$ materials is still lacking. In bulk materials the first problem to be considered is their high porosity, ascribed to the densification problems previously described. However, even for highly dense ($\rho > 95\ \%\ \rho_t$) bulk materials [95, 101] or thin films [129, 134, 135], the problems with the high conductivity still persist. Some authors attribute the origin of this high electrical conductivity to the presence of secondary phases [135, 136], although some others consider the defect structure, namely oxygen vacancies and / or iron ions in the 2+ oxidation state [134, 137], as the main responsible of such high conductivity values. Working with thin films Bèa et al. [135], realized that the Bi_2O_3 secondary phase can create conduction pathways through the material resulting in a high electrical conductivity. The same effect could be expected from the Bi-rich secondary phase, $Bi_{25}FeO_{39}$, with a sillenite-type structure quite similar to that of Bi_2O_3. On the other hand, Lahmar et al. [136] deposited thin films from a $BiFeO_3$ composition containing a 10 % iron excess by spin-coating and estimated that the presence of γ-Fe_2O_3 parasitic phase was behind the observed increase in the electrical conductivity. These authors also proposed that the electrical conductivity in single-phase $BiFeO_3$ films is originated by the oxygen vacancies and it may be decreased by shifting the nominal composition either towards a 10 % Bi_2O_3 enriched composition (preexistent bismuth vacancies due to volatilization would be occupied by Bi^{3+} ions, and hence O^{2-} species would be released annihilating the oxygen vacancies) or towards compositions containing up to 5 % Fe_2O_3 excess (so Fe^{3+} ions may occupy the bismuth vacancies also releasing O^{2-} that annihilate oxygen vacancies). In contrast, Ke et al. [137] suggested that the high electrical conductivity must be ascribed to the existence of Fe^{2+} ions rather than to the presence of oxygen vacancies or secondary phases (excepting the case in which these phases are present in macroscopic amounts). These authors performed a structural study on bulk $BiFeO_3$ ceramics sintered under different atmospheres (either Ar or O_2), and observed that the dielectric looses were higher for the ceramics sintered in Ar. Thus, by leaning on XPS analyses, these authors attributed the higher conductivity to a higher proportion of Fe^{2+}.

But besides when $BiFeO_3$ materials are doped in A or B positions with small amounts of different ions, significant changes can be promoted in their properties due to the effect that these dopant may have on stabilizing the α-$BiFeO_3$ phase, on the densification mechanisms and on the defect chemistry. However, once more, the literature shows a lot of controversy regarding the properties of $BiFeO_3$-doped materials. This must be attributed to the high sensitivity of $BiFeO_3$ materials to the experimental parameters during processing, but also to the

Table I. Measured values for the polarization of $BiFeO_3$ in several published works, in chronological order, showing the disparity of values.

Ref.	Publication year	Sample type	P ($\mu C/cm^2$)
[155]	1970	Bulk single crystals	6.1
[154]	1999	$(Bi_{0.7}Ba_{0.3})(Fe_{0.7}Ti_{0.3})O_3$ films (300 nm) on Nb-doped $SrTiO_3$	2.5
[20]	2003	Thin films (400–100 nm) on $SrRuO_3$ /$SrTiO_3$	50-60
[153]	2003	Polycrystalline films (300 nm)	35.7
[152]	2004	Polycrystalline films (300 nm)	158
[149]	2005	Bulk ceramics	23.5
[150]	2006	Thin films (200 nm) on $SrRuO_3$ /$SrTiO_3$	86-98

fact that many works lack of a suitable characterization of the materials (as mentioned, it is quite common to assume a pure phase by just leaning on X-ray diffraction measurements). Also misinterpretations of the experimental data are frequent, like when rounded ferroelectric loops are used for asserting changes in the concentration of defects, as described above.

Doping with cations that can stabilize the perovskite phase could be an effective method to decrease the electrical conductivity of the $BiFeO_3$ materials. Some authors suggest that La^{3+} doping can decrease the electrical conductivity [107, 138]. An enhancement in the electric polarization of $Bi_{1-x}La_xFeO_3$ materials has as well been reported [107, 108], although no saturated cycles (that can confirm this effect) are provided. In clear disagreement with these publications, some other authors however assert that although the dielectric losses decrease upon doping with rare-earth elements in A sites, the substitution of a certain amount of Bi^{3+} ions finally tend to weaken the stereochemical activity of the s^2 lone pair of Bi^{3+} (whose hybridation gives rise to ferroelectricity) thereby resulting in a paraelectric behavior [58, 59].

On the other hand, aliovalent dopants will strongly influence the electric properties of $BiFeO_3$ materials, as a consequence of changes in the chemistry of defects. According to Mazumder et al. [117], doping with Pb^{2+} decreases the electrical conductivity of $BiFeO_3$ and improves its polarization by decreasing the Fe^{2+} concentration. Doping with Zn^{2+} [139], Co^{2+} or Cu^{2+} [140] has also been reported to decrease the leakage current of $BiFeO_3$ materials. However, many other works propose that the electrical conductivity of bismuth ferrite materials rises upon substitution with acceptor dopants. For example, Qui et al. [121] asserted that doping with Ni^{2+} increases the conductivity by means of a vacancy conduction mechanism. According to Khomchenko et al. [119], doping with Pb^{2+}, Ca^{2+}, Sr^{2+} or Ba^{2+} increases the oxygen vacancy concentration –which is supported by Mössbauer spectroscopy- and thus increases the electrical conductivity. On the other hand, Moure et al. [101] suggest that doping $BiFeO_3$ with Sr^{2+} increases the grain boundary conductivity.

With regards to donor dopants there is a more generalized agreement about their effect in decreasing the electrical conductivity. For example, it has been several times reported in literature that doping with Nb^{5+} decreases the electrical conductivity of $BiFeO_3$ materials [66, 118, 141]. However, the reasons for this lower conductivity of the doped material have been ascribed to different factors such as a decrease in the oxygen vacancies concentration or a possible niobium segregation at the grain boundaries. The case is that ferroelectric loops have been measured just for Nb-doped $BiFeO_3$ materials conformed as thin films and, up to date, results are contradictory. For example, whereas some works assert an enhancement of the remnant polarization in comparison with undoped $BiFeO_3$ thin films prepared by similar methods [141] (although saturated ferroelectric loops are never obtained in those cases), others support that remnant polarization falls off with niobium doping [142]. Apart from niobium, doping with Ti^{4+} in the Fe^{3+} positions is also a common method used to decrease the electrical conductivity in $BiFeO_3$ materials [61, 62, 121, 122], although once again some works describe just the opposite effect [139]. In fact, there is not a generalized agreement regarding the charge compensation mechanisms; [61, 122, 143] in this context, it has been recently suggested that the charge compensation mechanism in Ti-doped $BiFeO_3$ ceramics may shift from an electronic compensation mechanism in the grain interior to a vacancy compensation mechanism in the grain boundary due to Ti^{4+} segregation, this having a key role in the multiferroic properties [62]. Finally, Zr^{4+} [144], V^{5+} [145] or W^{6+} [146] are other donor-like dopants which have been used to improve the ferroelectric properties of $BiFeO_3$ materials. However, in spite of the reported improvements in the dielectric properties, ferroelectric loops are still not saturated.

On the other hand, doping at the Fe^{3+} positions with manganese is also very common in the literature of $BiFeO_3$ materials. Some authors suggest that small amounts of this dopant decrease the electrical conductivity of $BiFeO_3$ materials [140, 147], but some others describe an increase in conductivity with the increase in the amount of manganese [60, 141, 148]. For example, Selbach et al. [60] reported that, since $BiFeO_3$ is a p-type semiconductor, doping with Mn^{3+} will lead to an increase of the electrical conductivity because the oxygen hyper-stoichiometry produced by the partial oxidation of Mn^{3+} to Mn^{4+} rises the concentration of cationic vacancies.

Among the large amount of published works, saturated ferroelectric cycles have been occasionally reported for $BiFeO_3$ materials, both in bulk [149] and in thin films [20, 150-154]. Also the reported remnant polarization values are very variable (**table I**). In the case of bulk materials, the highest value reported up to date is about 12 $\mu C/cm^2$ [149], whereas for thin films those values are up to one order of magnitude higher [20] although the reasons for this high values are still not clear [134].

In summary, the literature of $BiFeO_3$ based materials shows plenty of results which are poorly reproducible. Thus, it is possible to find works that describe completely different properties in samples prepared with similar procedures. The

disparity in the polarization values could be due to different reasons, from a high electrical conductivity in bulk samples [21] to strain-stabilized structural modifications in thin films [20]. Nevertheless, the effect of stress on the increase of the remnant polarization in thin films has been later refused by different authors as Erenstein et al. [134] o Ederer et al. [156]. Using the modern theory of polarization, some theoretical studies allow explaining both the unexpected low values and those anomaly large which have been recently obtained considering structures in which the ions can shift their oxidation state [21]. However, these theoretical results have not been experimentally verified due to problems related with the synthesis and the characterization of the $BiFeO_3$ materials [21].

7.2. Magnetic response in $BiFeO_3$ materials

As previously explained, $BiFeO_3$ crystals with a size longer than the spin cycloid wavelength, i.e. 64 nm, show an anti-ferromagnetic behavior. However, this superstructure can be frustrated leading to a ferrimagnetic response, something which has been pursued by different strategies: applying high magnetic fields (~ 20 T), reducing the particle size, introducing restrictions in thin films or by chemical substitution [2, 157, 158].

In 2003 Wang et al. [20] reported an extraordinary large magnetization value (M_s ~150 emu/g, i.e. ~ 1 μ_B/Fe) for epitaxial $BiFeO_3$ thin films with a thickness of 70 nm. The authors attributed this anomalous enhancement of magnetization (which depended on the film thickness) to strain. However, years later several authors have refuted this hypothesis concluding that the magnetic response was actually independent on the film thickness [25, 134] and suggesting that the high magnetization value could be attributed to Fe^{2+} ions [134] or to small amounts of the γ-Fe_2O_3 secondary phase [25].

It has also been reported that $BiFeO_3$ nanoparticles smaller than ~ 92 nm in size show an enhancement in magnetization strongly dependent on the particle size [158-161]. This improvement in magnetization has been related with the frustration of anti-ferromagnetism in reduced size particles as well as with the presence of decompensate spins and anisotropic stresses in the surface of the nanoparticles [159]. In 2007, Mazumder et al. [158] reported a magnetization of ~ 0.4 μ_B/Fe for $BiFeO_3$ nanoparticles with a size of 4 nm, a considerably high value in comparison with that obtained for bulk samples ~ 0.02 μ_B/Fe. However, samples with similar sizes obtained through different synthesis methods yielded different magnetization and coercivity values [159, 162]. This last fact suggests that the magnetic properties of $BiFeO_3$ nanoparticles also depend on the processing story [162].

Chemical substitution has also been used quite frequently in order to improve the magnetization in $BiFeO_3$ materials. Substitution of Bi^{3+} ions in A sites by diamagnetic ions like La^{3+}, Sr^{2+}, Pb^{2+} or Ba^{2+} results in an enhancement of the magnetization which can be correlated with the ionic radius of the substituting dopant [119, 163]. Khomchenko et al. [119] suggested that the enlargement in magnetization when substituting with a diamagnetic dopant is due to the variation on the anisotropic constant. However, other authors support that such increase in magnetization for Ba^{2+} doped $BiFeO_3$ materials is due either to the increasing in the Fe^{2+} concentration when dealing with thin films [114] or to a different balance of the oxygen vacancies in the case of bulk $BiFeO_3$ ceramics [164].

Finally it has also been published that doping in B sites of the perovskite structure may lead to an enhancement in magnetization, since the substitution of iron atoms can increase the value of the Fe-O-Fe angle and, hence, modify the super-exchange interaction [165]. As reported, dopants like Ti^{4+} [61, 122, 143, 166], Nb^{5+} [118, 167] o Zr^{4+} [168] can originate a weak ferromagnetism in $BiFeO_3$ materials.

8. CONCLUSIONS

In the last decade a great effort has been done regarding the synthesis and the obtaining of multiferroic $BiFeO_3$-based materials. However, among the large amount of published papers there is still much controversy which is mainly due to the difficulties in preparation and characterization of $BiFeO_3$ materials. The published phase diagrams for the Bi_2O_3-Fe_2O_3 system show contradictory data and not even the thermodynamic nature of the $BiFeO_3$ phase is clear in literature. Synthesis of a pure $BiFeO_3$ phase is tricky and usually results in the presence of a certain amount of secondary phases. A scarce characterization may overlook the parasite phases leading to contradictory results and poorly reproducible properties. Besides, misinterpretations of the obtained data, such as ferroelectric loops typical of highly conductive materials, also frequently lead to erroneous conclusions. The result is a misunderstanding in the origin of the observed properties which, on the other hand, are habitually interesting for applications of $BiFeO_3$ multiferroics. Thus, works regarding $BiFeO_3$ materials must be critically considered with these key points in mind and taking into account their experimental procedures as well as the thoroughness of their characterization. Only in this way, practical applications of $BiFeO_3$ multiferroics could be reached, which is in fact a truly challenge for materials research.

ACKNOWLEDGES

This work has been conducted within the CICYT MAT 2010-16614 project and the FPU program (AP2008-00053) of the Spanish Ministry of Education. Author also acknowledges Dr. A.C. Caballero, Dr. T. Jardiel and Dr. M. Peiteado for support.

REFERENCES

1. Martin, L. W.; Crane, S. P.; Chu, Y. H.; Holcomb, M. B.; Gajek, M.; Huijben, M.; Yang, C. H.; Balke, N.; Ramesh, R., (2008): Multiferroics and magnetoelectrics: Thin films and nanostructures. *J. Phys-Condens. Mat.*, **20** (43): 434220.
2. Eerenstein, W.; Mathur, N. D.; Scott, J. F., (2006): Multiferroic and magnetoelectric materials. *Nature*, **442** (7104): 759-765.
3. Schmid, H. *On ferrotoroidics and electrotoroidic, magnetotoroidic and piezotoroidic effects*. 2001. Nanjing.
4. Ma, J.; Hu, J.; Li, Z.; Nan, C. W., (2011): Recent progress in multiferroic magnetoelectric composites: From bulk to thin films. *Adv. Mater.*, **23** (9): 1062-1087.
5. Spaldin, N. A.; Fiebig, M., (2005): The renaissance of magnetoelectric multiferroics. *Science*, **309** (5733): 391-392.
6. Yatom, H.; Englman, R., (1969): Theoretical methods in the magnetoelectric effect. I. Formal treatment. *Phys. Rev.*, **188** (2): 793-802.
7. Fiebig, M., (2005): Revival of the magnetoelectric effect. *J. Phys. D Appl. Phys.*, **38** (8): R123-R152.

8. Bibes, M.; Barthélémy, A., (2008): Multiferroics: Towards a magnetoelectric memory. *Nat. Mater.*, **7** (6): 425-426.
9. Scott, J. F., (2007): Data storage: Multiferroic memories. *Nat. Mater.*, **6** (4): 256-257.
10. Ascher, E.; Rieder, H.; Schmid, H.; Stössel, H., (1966): Some properties of ferromagnetoelectric nickel-iodine boracite, $Ni_3B_7O_{13}I$. *J. Appl. Phy.*, **37** (3): 1404-1405.
11. Hill, N. A., (2000): Why are there so few magnetic ferroelectrics? *J. Phys. Chem. B*, **104** (29): 6694-6709.
12. Cohen, R. E., (1992): Origin of ferroelectricity in perovskite oxides. *Nature*, **358** (6382): 136-138.
13. Ederer, C.; Spaldin, N. A., (2004): A new route to magnetic ferroelectrics. *Nat. Mater.*, **3** (12): 849-851.
14. Scott, J. F.; Blinc, R., (2011): Multiferroic magnetoelectric fluorides: Why are there so many magnetic ferroelectrics? *J. Phys-Condens. Mat.*, **23** (11): 113202.
15. Van Aken, B. B.; Palstra, T. T. M.; Filippetti, A.; Spaldin, N. A., (2004): The origin of ferroelectricity in magnetoelectric $YMnO_3$. *Nat. Mater.*, **3** (3): 164-170.
16. Kimura, T.; Goto, T.; Shintani, H.; Ishizaka, K.; Arima, T.; Tokura, Y., (2003): Magnetic control of ferroelectric polarization. *Nature*, **426** (6962): 55-58.
17. Hur, N.; Park, S.; Sharma, P. A.; Ahn, J. S.; Guha, S.; Cheong, S. W., (2004): Electric polarization reversal and memory in a multiferroic material induced by magnetic fields. *Nature*, **429** (6990): 392-395.
18. Mitoseriu, L., (2005): Magnetoelectric phenomena in single-phase and composite systems. *Bol. Soc. Esp. de Ceram. V.*, **44**: 177-184.
19. Hill, N. A., (2002): Density functional studies of multiferroic magnetoelectrics. *Annu. Rev. Mater. Sci.*, **32**: 1-37.
20. Wang, J.; Neaton, J. B.; Zheng, H.; Nagarajan, V.; Ogale, S. B.; Liu, B.; Viehland, D.; Vaithyanathan, V.; Schlom, D. G.; Waghmare, U. V.; Spaldin, N. A.; Rabe, K. M.; Wuttig, M.; Ramesh, R., (2003): Epitaxial $BiFeO_3$ multiferroic thin film heterostructures. *Science*, **299** (5613): 1719-1722.
21. Neaton, J. B.; Ederer, C.; Waghmare, U. V.; Spaldin, N. A.; Rabe, K. M., (2005): First-principles study of spontaneous polarization in multiferroic $BiFeO_3$. *Phys. Rev. B*, **71** (1): 014113.
22. Catalan, G.; Scott, J. F., (2009): Physics and applications of bismuth ferrite. *Adv. Mater.*, **21** (24): 2463-2485.
23. Naganuma, H., *Chapter 16. Multifunctional Characteristics of B-site Substituted $BiFeO_3$ Films*, in *Ferroelectrics - Physical Effects*, M. Lallart, Editor 2011. p. 654.
24. Selbach, S. M.; Tybell, T.; Einarsrud, M. A.; Grande, T., (2007): Size-dependent properties of multiferroic $BiFeO_3$ nanoparticles. *Chem. Mater.*, **19** (26): 6478-6484.
25. Béa, H.; Bibes, M.; Fusil, S.; Bouzehouane, K.; Jacquet, E.; Rode, K.; Bencok, P.; Barthélémy, A., (2006): Investigation on the origin of the magnetic moment of $BiFeO_3$ thin films by advanced x-ray characterizations. *Phys. Rev. B*, **74** (2): 020101(R).
26. Wang, H.; Yang, C.; Lu, J.; Wu, M.; Su, J.; Li, K.; Zhang, J.; Li, G.; Jin, T.; Kamiyama, T.; Liao, F.; Lin, J.; Wu, Y., (2013): On the structure of □-$BiFeO_3$. *Inorganic Chemistry*, **52** (5): 2388-2392.
27. Zhao, T.; Scholl, A.; Zavaliche, F.; Lee, K.; Barry, M.; Doran, A.; Cruz, M. P.; Chu, Y. H.; Ederer, C.; Spaldin, N. A.; Das, R. R.; Kim, D. M.; Baek, S. H.; Eom, C. B.; Ramesh, R., (2006): Electrical control of antiferromagnetic domains in multiferroic $BiFeO_3$ films at room temperature. *Nat. Mater.*, **5** (10): 823-829.
28. Prellier, W.; Singh, M. P.; Murugavel, P., (2005): The single-phase multiferroic oxides: From bulk to thin film. *J. Phys-Condens. Mat.*, **17** (30): R803-R832.
29. Lebeugle, D.; Colson, D.; Forget, A.; Viret, M.; Bonville, P.; Marucco, J. F.; Fusil, S., (2007): Room-temperature coexistence of large electric polarization and magnetic order in $BiFeO_3$ single crystals. *Phys. Rev. B*, **76** (2): 024116.
30. Sosnowska, I.; Neumaier, T. P.; Steichele, E., (1982): Spiral magnetic ordering in bismuth ferrite. *J. Phys. C Solid State*, **15** (23): 4835-4846.
31. Moreau, J. M.; Michel, C.; Gerson, R.; James, W. J., (1971): Ferroelectric $BiFeO_3$ X-Ray and Neutron Diffraction Study. *J. Phys. Chem. Solids*, **32** (6): 1315-1320.
32. Selbach, S. M.; Tybell, T.; Einarsrud, M. A.; Grande, T., (2008): The ferroic phase transitions of $BiFeO_3$. *Adv. Mater.*, **20** (19): 3692-3696.
33. Lu, J.; Qiao, L. J.; Fu, P. Z.; Wu, Y. C., (2011): Phase equilibrium of Bi_2O_3-Fe_2O_3 pseudo-binary system and growth of $BiFeO_3$ single crystal. *J. Cryst. Growth*, **318** (1): 936-941.
34. Polomska, M.; Kaczmarek, W.; Pajak, Z., (1974): Electric and magnetic properties of $(Bi_{1-x}La_x)FeO_3$ solid solutions. *Physica Status Solidi (A) Applied Research*, **23** (2): 567-574.
35. Palai, R.; Katiyar, R. S.; Schmid, H.; Tissot, P.; Clark, S. J.; Robertson, J.; Redfern, S. a. T.; Catalan, G.; Scott, J. F., (2008): β–phase and β-γ metal-insulator transition in multiferroic $BiFeO_3$. *Phys. Rev. B*, **77** (1): 014110.
36. Haumont, R.; Kornev, I. A.; Lisenkov, S.; Bellaiche, L.; Kreisel, J.; Dkhil, B., (2008): Phase stability and structural temperature dependence in powdered multiferroic $BiFeO_3$. *Phys. Rev. B*, **78** (13): 134108.
37. Arnold, D. C.; Knight, K. S.; Morrison, F. D.; Lightfoot, P., (2009): Ferroelectric-paraelectric transition in $BiFeO_3$: Crystal structure of the orthorhombic □ phase. *Phys. Rev. Lett.*, **102** (2): 027602.
38. Selbach, S. M.; Tybell, T.; Einarsrud, M.-A.; Grande, T., (2010): Phase transitions, electrical conductivity and chemical stability of BiFeO3 at high temperatures. *J. Solid State Chem.*, **183** (5): 1205-1208.
39. Speranskaya, E. I.; Skorikov, V. M.; Rode, E. Y.; Terekhova, V. A., (1966): The phase diagram of the system bismuth oxide-ferric oxide. *B. Acad. Sci. USSR Ch+*, **14** (5): 873-874.
40. Morozov, M. I.; Lomanova, N. A.; Gusarov, V. V., (2003): Specific features of $BiFeO_3$ formation in a mixture of bismuth(III) and iron(III) oxides. *Russ. J. Gen. Chem.*, **73** (11): 1676-1680.
41. Maitre, A.; Francois, M.; Gachon, J. C., (2004): Experimental study of the Bi_2O_3-Fe_2O_3 pseudo-binary system. *J. Phase Equilib. Diff.*, **25** (1): 59-67.
42. Achenbac.G. D.; James, W. J.; Gerson, R., (1967): Preparation of single-phase polycrystalline $BiFeO_3$. *J. Am. Ceram. Soc.*, **50** (8): 437.
43. Valant, M.; Axelsson, A. K.; Alford, N., (2007): Peculiarities of a solid-state synthesis of multiferroic polycrystalline $BiFeO_3$. *Chem. Mater.*, **19**: 5431-5436.
44. Carvalho, T. T.; Tavares, P. B., (2008): Synthesis and thermodynamic stability of multiferroic $BiFeO_3$. *Mater. Lett.*, **62** (24): 3984-3986.
45. Selbach, S. M.; Einarsrud, M. A.; Grande, T., (2009): On the Thermodynamic Stability of $BiFeO_3$. *Chem. Mater.*, **21** (1): 169-173.
46. Smolenskii, A.; Agranovskaya, A. I.; Popov, S. N.; Isupov, V. A., (1958): *Sov. Phys-Tech. Phys.*, **3**: 1981.
47. Dai, Z.-H.; Akishige, Y., (2012): $BiFeO_3$ ceramics synthesized by spark plasma sintering. *Ceram. Int.*, **38** (1): 403-406.
48. Wang, Y. P.; Zhou, L.; Zhang, M. F.; Chen, X. Y.; Liu, J. M.; Liu, Z. G., (2004): Room-temperature saturated ferroelectric polarization in $BiFeO_3$ ceramics synthesized by rapid liquid phase sintering. *Appl. Phys. Lett.*, **84** (10): 1731-1733.
49. Pradhan, A. K.; Zhang, K.; Hunter, D.; Dadson, J. B.; Loiutts, G. B.; Bhattacharya, P.; Katiyar, R.; Zhang, J.; Sellmyer, D. J.; Roy, U. N.; Cui, Y.; Burger, A., (2005): Magnetic and electrical properties of single-phase multiferroic $BiFeO_3$. *J. Appl. Phy.*, **97** (9): 1-4.
50. Yuan, G. L.; Or, S. W.; Wang, Y. P.; Liu, Z. G.; Liu, J. M., (2006): Preparation and multi-properties of insulated single-phase $BiFeO_3$ ceramics. *Solid State Commun.*, **138**: 76-81.
51. Bernardo, M. S.; Jardiel, T.; Peiteado, M.; Caballero, A. C.; Villegas, M., (2011): Reaction pathways in the solid state synthesis of multiferroic BiFeO3. *J. Eur. Ceram. Soc.*, **31** (16): 3047-3053.
52. Karimi, S.; Reaney, I. M.; Han, Y.; Pokorny, J.; Sterianou, I., (2009): Crystal chemistry and domain structure of rare-earth doped $BiFeO_3$ ceramics. *J. Mater. Sci.*, **44** (19): 5102-5112.
53. Cheng, Z. X.; Li, A. H.; Wang, X. L.; Dou, S. X.; Ozawa, K.; Kimura, H.; Zhang, S. J.; Shrout, T. R., (2008): Structure, ferroelectric properties, and magnetic properties of the La-doped bismuth ferrite. *J. Appl. Phy.*, **103** (7): 07E507.
54. Uniyal, P.; Yadav, K. L., (2008): Study of dielectric, magnetic and ferroelectric properties in $Bi_{1-x}Gd_xFeO_3$. *Mater. Lett.*, **62** (17-18): 2858-2861.
55. Nalwa, K. S.; Garg, A.; Upadhyaya, A., (2008): Effect of samarium doping on the properties of solid-state synthesized multiferroic bismuth ferrite. *Mater. Lett.*, **62** (6-7): 878-881.
56. Minh, N. V.; Thang, D. V., (2010): Dopant effects on the structural, optical and electromagnetic properties in multiferroic $Bi_{1-x}Y_xFeO_3$ ceramics. *J. Alloys Compd.*, **505** (2): 619-622.
57. Van Minh, N.; Gia Quan, N., (2011): Structural, optical and electromagnetic properties of $Bi_{1-x}Ho_xFeO_3$ multiferroic materials. *J. Alloys Compd.*, **509** (6): 2663-2666.
58. Yuan, G. L.; Or, S. W.; Liu, J. M.; Liu, Z. G., (2006): Structural transformation and ferroelectromagnetic behavior in single-phase $Bi_{1-x}Nd_xFeO_3$ multiferroic ceramics. *Appl. Phys. Lett.*, **89** (5): 052905.
59. Uchida, H.; Ueno, R.; Funakubo, H.; Koda, S., (2006): Crystal structure and ferroelectric properties of rare-earth substituted $BiFeO_3$ thin films. *J. Appl. Phy.*, **100** (1): 014106.
60. Selbach, S. M.; Tybell, T.; Einarsrud, M. A.; Grande, T., (2009): Structure and properties of multiferroic oxygen hyperstoichiometric $BiFe_{1-x}Mn_xO_{3+\delta}$. *Chem. Mater.*, **21** (21): 5176-5186.
61. Kim, S. J.; Han, S. H.; Kim, H. G.; Kim, A. Y.; Kim, J. S.; Cheon, C. I., (2010): Multiferroic properties of Ti-doped $BiFeO_3$ ceramics. *J.Korean Phys.l Soc.*, **56** (12): 439-442.
62. Bernardo, M. S.; Jardiel, T.; Peiteado, M.; Mompean, F. J.; Garcia-Hernandez, M.; Garcia, M. A.; Villegas, M.; Caballero, A. C., (2013): Intrinsic compositional inhomogeneities in bulk Ti-doped $BiFeO_3$: Microstructure development and multiferroic properties. *Chem. Mater.*, **25** (9): 1533-1541.
63. Bernardo, M. S.; Jardiel, T.; Peiteado, M.; Caballero, A. C.; Villegas, M., (2011): Sintering and microstuctural characterization of W^{6+}, Nb^{5+} and Ti^{4+} iron-substituted $BiFeO_3$. *J. Alloys Compd.*, **509** (26): 7290-7296.
64. Azough, F.; Freer, R.; Thrall, M.; Cernik, R.; Tuna, F.; Collison, D., (2009): Microstructure and properties of Co-, Ni-, Zn-, Nb- and W-modified multiferroic $BiFeO_3$ ceramics. *J. Eur. Ceram. Soc.*, **30** (3): 727-736.

65. Bernardo, M. S.; Jardiel, T.; Villegas, M., (2010): Synthesis and microstructural evolution of $BiFeO_3$ ceramics modified with ZnO. *Bol. Soc. Esp. de Ceram. V.*, **49** (1): 47-52.
66. Jun, Y. K.; Hong, S. H., (2007): Dielectric and magnetic properties in Co- and Nb-substituted $BiFeO_3$ ceramics. *Solid State Commun.*, **144** (7-8): 329-333.
67. Chen, J. C.; Wu, J. M., (2007): Dielectric properties and ac conductivities of dense single-phased $BiFeO_3$ ceramics. *Appl. Phys. Lett.*, **91** (18): 182903.
68. Ke, H.; Wang, W.; Wang, Y.; Xu, J.; Jia, D.; Lu, Z.; Zhou, Y., (2011): Factors controlling pure-phase multiferroic $BiFeO_3$ powders synthesized by chemical co-precipitation. *J. Alloys Compd.*, **509** (5): 2192-2197.
69. Kothai, V.; Ranjan, R., (2012): Synthesis of $BiFeO_3$ by carbonate precipitation. *B. Mater. Sci.*, **35** (2): 157-161.
70. Liu, Z.; Qi, Y.; Lu, C., (2010): High efficient ultraviolet photocatalytic activity of $BiFeO_3$ nanoparticles synthesized by a chemical coprecipitation process. *J. Mater. Sci-Mater El.*, **21** (4): 380-384.
71. Shami, M. Y.; Awan, M. S.; Anis-Ur-Rehman, M., (2011): Phase pure synthesis of $BiFeO_3$ nanopowders using diverse precursor via co-precipitation method. *J. Alloys Compd.*, **509** (41): 10139-10144.
72. Shetty, S.; Palkar, V. R.; Pinto, R., (2002): Size effect study in magnetoelectric $BiFeO_3$ system. *Pramana-J. Phys.*, **58** (5-6): 1027-1030.
73. Rahaman, N., (2007): *Ceramic Processing*, CRC/Taylor & Francis, New York.
74. Selbach, S. M.; Einarsrud, M. A.; Tybell, T.; Grande, T., (2007): Synthesis of $BiFeO_3$ by wet chemical methods. *J. Am. Ceram. Soc.*, **90**: 3430-3434.
75. Ghosh, S.; Dasgupta, S.; Sen, A.; Maiti, H. S., (2005): Low-temperature synthesis of nanosized bismuth ferrite by soft chemical route. *J. Am. Ceram. Soc.*, **88** (5): 1349-1352.
76. Popa, M.; Crespo, D.; Calderon-Moreno, J. M.; Preda, S.; Fruth, V., (2007): Synthesis and structural characterization of single-phase $BiFeO_3$ powders from a polymeric precursor. *J. Am. Ceram. Soc.*, **90** (9): 2723-2727.
77. Wang, X.; Zhang, Y.; Wu, Z., (2010): Magnetic and optical properties of multiferroic bismuth ferrite nanoparticles by tartaric acid-assisted sol-gel strategy. *Mater. Lett.*, **64** (3): 486-488.
78. Park, T. J.; Mao, Y.; Wong, S. S., (2004): Synthesis and characterization of multiferroic $BiFeO_3$ nanotubes. *Chem. Commun.*, (23): 2708-2709.
79. Yoshimura, M.; Byrappa, K., (2008): Hydrothermal processing of materials: Past, present and future. *J. Mater. Sci.*, **43** (7): 2085-2103.
80. Han, J. T.; Huang, Y. H.; Wu, X. J.; Wu, C. L.; Wei, W.; Peng, B.; Huang, W.; Goodenough, J. B., (2006): Tunable synthesis of bismuth ferrites with various morphologies. *Adv. Mater.*, **18** (16): 2145-2148.
81. Chen, C.; Cheng, J. R.; Yu, S. W.; Che, L. J.; Meng, Z. Y., (2006): Hydrothermal synthesis of perovskite bismuth ferrite crystallites. *J. Cryst. Growth*, **291** (1): 135-139.
82. Wang, Y. G.; Xu, G.; Ren, Z. H.; Wei, X.; Weng, W. J.; Du, P.; Shen, G.; Han, G. R., (2007): Mineralizer-assisted hydrothermal synthesis and characterization of $BiFeO_3$ nanoparticles. *J. Am. Ceram. Soc.*, **90**: 2615-2617.
83. Wang, Y. G.; Xu, G.; Yang, L. L.; Ren, Z. H.; Wei, X.; Weng, W. J.; Du, P.; Shen, G.; Han, G. R., (2007): Alkali metal ions-assisted controllable synthesis of bismuth ferrites by a hydrothermal method. *J. Am. Ceram. Soc.*, **90**: 3673-3675.
84. Jiang, H.; Morozumi, Y.; Kumada, N.; Yonesaki, Y.; Takei, T.; Kinomura, N., (2008): Hydrothermal synthesis of perovskite-type $BiFeO_3$. *J. Ceram. Soc. Jpn.*, **116** (1355): 837-839.
85. Han, S. H.; Kim, K. S.; Kim, H. G.; Lee, H. G.; Kang, H. W.; Kim, J. S.; Cheon, C. I., (2010): Synthesis and characterization of multiferroic $BiFeO_3$ powders fabricated by hydrothermal method. *Ceram. Int.*, **36** (4): 1365-1372.
86. Gajovic, A.; Sturm, S.; Jancar, B.; Santic, A.; Zagar, K.; Ceh, M., (2010): The synthesis of pure-phase bismuth ferrite in the Bi-Fe-O system under hydrothermal conditions without a mineralizer. *J. Am. Ceram. Soc.*, **93** (10): 3173-3179.
87. Chen, X. Z.; Qiu, Z. C.; Zhou, J. P.; Zhu, G.; Bian, X. B.; Liu, P., (2011): Large-scale growth and shape evolution of bismuth ferrite particles with a hydrothermal method. *Mater. Chem. Phys.*, **126** (3): 560-567.
88. Xiaomeng, L. Ä.; Jimin, X.; Yuanzhi, S.; Jiamin, L., (2007): Surfactant-assisted hydrothermal preparation of submicrometer-sized two-dimensional $BiFeO_3$ plates and their photocatalytic activity. *J. Mater. Sci.*, **42** (16): 6824-6827.
89. Cho, C. M.; Noh, J. H.; Cho, I. S.; An, J. S.; Hong, K. S.; Kim, J. Y., (2008): Low-temperature hydrothermal synthesis of pure $BiFeO_3$ nanopowders using triethanolamine and their applications as visible-light photocatalysts. *J. Am. Ceram. Soc.*, **91** (11): 3753-3755.
90. Li, S.; Lin, Y. H.; Zhang, B. P.; Wang, Y.; Nan, C. W., (2010): Controlled fabrication of $BiFeO_3$ uniform microcrystals and their magnetic and photocatalytic behaviors. *J. Phys. Chem. C*, **114** (7): 2903-2908.
91. Huo, Y.; Jin, Y.; Zhang, Y., (2010): Citric acid assisted solvothermal synthesis of $BiFeO_3$ microspheres with high visible-light photocatalytic activity. *J. Mol. Catal. A-Chem*, **331** (1-2): 15-20.
92. Prado-Gonjal, J.; Villafuerte-Castrejón, M. E.; Fuentes, L.; Morán, E., (2009): Microwave-hydrothermal synthesis of the multiferroic $BiFeO_3$. *Mater. Res. Bull.*, **44** (8): 1734-1737.
93. Prado-Gonjal, J.; Ávila, D.; Villafuerte-Castrejón, M. E.; González-García, F.; Fuentes, L.; Gómez, R. W.; Pérez-Mazariego, J. L.; Marquina, V.; Morán, E., (2011): Structural, microstructural and Mössbauer study of $BiFeO_3$ synthesized at low temperature by a microwave-hydrothermal method. *Solid State Sci.*, **13** (11): 2030-2036.
94. Li, S.; Nechache, R.; Davalos, I. a. V.; Goupil, G.; Nikolova, L.; Nicklaus, M.; Laverdiere, J.; Ruediger, A.; Rosei, F., (2013): Ultrafast Microwave Hydrothermal Synthesis of $BiFeO_3$ Nanoplates. *J. Am. Ceram. Soc.*, **96** (10): 3155-3162.
95. Liu, H.; Pu, Y.; Shi, X.; Yuan, Q., (2012): Dielectric and ferroelectric properties of $BiFeO_3$ ceramics sintered in different atmospheres. *Ceram. Int.*, **39** (1): Pages S217–S220.
96. Kong, L. B.; Zhang, T. S.; Ma, J.; Boey, F., (2008): Progress in synthesis of ferroelectric ceramic materials via high-energy mechanochemical technique. *Prog. Mater. Sci.*, **53** (2): 207-322.
97. Szafraniak, I.; Polomska, M.; Hilczer, B.; Pietraszko, A.; Kepinski, L., (2007): Characterization of $BiFeO_3$ nanopowder obtained by mechanochemical synthesis. *J. Eur. Ceram. Soc.*, **27** (13-15): 4399-4402.
98. Da Silva, K. L.; Menzel, D.; Feldhoff, A.; Kã¼Bel, C.; Bruns, M.; Paesano, A.; Düvel, A.; Wilkening, M.; Ghafari, M.; Hahn, H.; Litterst, F. J.; Heitjans, P.; Becker, K. D.; Sepelák, V., (2011): Mechanosynthesized $BiFeO_3$ nanoparticles with highly reactive surface and enhanced magnetization. *J. Phys. Chem. C*, **115** (15): 7209-7217.
99. Freitas, V. F.; Grande, H. L. C.; De Medeiros, S. N.; Santos, I. A.; Cótica, L. F.; Coelho, A. A., (2008): Structural, microstructural and magnetic investigations in high-energy ball milled $BiFeO_3$ and $Bi_{0.95}Eu_{0.05}FeO_3$ powders. *J. Alloys Compd.*, **461** (1-2): 48-52.
100. Maurya, D.; Thota, H.; Garg, A.; Pandey, B.; Chand, P.; Verma, H. C., (2009): Magnetic studies of multiferroic $Bi_{1-x}Sm_xFeO_3$ ceramics synthesized by mechanical activation assisted processes. *J. Phys-Condens. Mat.*, **21** (2): 026007.
101. Moure, A.; Tartaj, J.; Moure, C., (2011): Processing and characterization of Sr doped $BiFeO_3$ multiferroic materials by high energetic milling. *J. Alloys Compd.*, **509** (25): 7042-7046.
102. Saravana Kumar, K.; Venkateswaran, C.; Kannan, D.; Tiwari, B.; Ramachandra Rao, M. S., (2012): Mechanical milling assisted synthesis of Ba-Mn co-substituted $BiFeO_3$ ceramics and their properties. *J. Phys. D Appl. Phys.*, **45** (41): 415302.
103. Correas, C.; Hungría, T.; Castro, A., (2011): Mechanosynthesis of the whole $xBiFeO_3$-(1 - X)$PbTiO_3$ multiferroic system: Structural characterization and study of phase transitions. *J. Mater. Chem.*, **21** (9): 3125-3132.
104. Dai, Z.; Akishige, Y., (2012): Electrical properties of $BiFeO_3$-$BaTiO_3$ ceramics fabricated by mechanochemical synthesis and spark plasma sintering. *Mater. Lett.*, **88**: 36-39.
105. Kingery, W. D.; Bowen, H. K.; Uhlmann, D. R., (1976): *Introduction to ceramics*, Wiley, New York - Chichester - Brisbane - Toronto - Singapur
106. Chen, F.; Zhang, Q. F.; Li, J. H.; Qi, Y. J.; Lu, C. J.; Chen, X. B.; Ren, X. M.; Zhao, Y., (2006): Sol-gel derived multiferroic $BiFeO_3$ ceramics with large polarization and weak ferromagnetism. *Appl. Phys. Lett.*, **89** (9): 092910.
107. Simões, A. Z.; Garcia, F. G.; Riccardi, C. D. S., (2009): Rietveld analysys and electrical properties of lanthanum doped $BiFeO_3$ ceramics. *Mater. Chem. Phys.*, **116** (2-3): 305-309.
108. Jiang, Q. H.; Nan, C. W.; Shen, Z. J., (2006): Synthesis and properties of multiferroic La-modified $BiFeO_3$ ceramics. *J. Am. Ceram. Soc.*, **89** (7): 2123-2127.
109. Mazumder, R.; Chakravarty, D.; Bhattacharya, D.; Sen, A., (2009): Spark plasma sintering of $BiFeO_3$. *Mater. Res. Bull.*, **44** (3): 555-559.
110. Jiang, Q. H.; Nan, C. W.; Wang, Y.; Liu, Y. H.; Shen, Z. J., (2008): Synthesis and properties of multiferroic $BiFeO_3$ ceramics. *J. Electroceram.*, **21** (1-4): 690-693.
111. Bertolino, N.; Garay, J.; Anselmi-Tamburini, U.; Munir, Z. A., (2001): Electromigration effects in Al-Au multilayers. *Scripta Mater.*, **44** (5): 737-742.
112. Kozakov, A. T.; Kochur, A. G.; Googlev, K. A.; Nikolsky, A. V.; Raevski, I. P.; Smotrakov, V. G.; Yeremkin, V. V., (2011): X-ray photoelectron study of the valence state of iron in iron-containing single-crystal ($BiFeO_3$, $PbFe_{1/2}Nb_{1/2}O_3$), and ceramic ($BaFe_{1/2}Nb_{1/2}O_3$) multiferroics. *J. Electron Spectrosc.*, **184** (1-2): 16-23.
113. Li, M.; Macmanus-Driscoll, J. L., (2005): Phase stability, oxygen nonstoichiometry and magnetic properties of $BiFeO_{3-\delta}$. *Appl. Phys. Lett.*, **87** (25): 1-3.
114. Yu, B.; Li, M.; Wang, J.; Hu, Z.; Liu, X.; Zhu, Y.; Zhao, X., (2012): Dependence of magnetic properties on the Fe^{2+} ion in Ba-doped $BiFeO_3$ multiferroic films. *Thin Solid Films*, **520** (11): 4089-4091.
115. Kumar, M.; Yadav, K. L.; Varma, G. D., (2008): Large magnetization and weak polarization in sol-gel derived $BiFeO_3$ ceramics. *Mater. Lett.*, **62** (8-9): 1159-1161.
116. Nalwa, K. S.; Garg, A., (2008): Phase evolution, magnetic and electrical properties in Sm-doped bismuth ferrite. *J. Appl. Phy.*, **103** (4): 044101.
117. Mazumder, R.; Sen, A., (2009): Effect of Pb-doping on dielectric properties of $BiFeO_3$ ceramics. *J. Alloys Compd.*, **475** (1-2): 577-580.
118. Jun, Y. K.; Moon, W. T.; Chang, C. M.; Kim, H. S.; Ryu, H. S.; Kim, J. W.; Kim, K. H.; Hong, S. H., (2005): Effects of Nb-doping on electric and magnetic properties in multi-ferroic $BiFeO_3$ ceramics. *Solid State Commun.*, **135** (1-2): 133-137.

119. Khomchenko, V. A.; Kiselev, D. A.; Kopcewicz, M.; Maglione, M.; Shvartsman, V. V.; Borisov, P.; Kleemann, W.; Lopes, A. M. L.; Pogorelov, Y. G.; Araujo, J. P.; Rubinger, R. M.; Sobolev, N. A.; Vieira, J. M.; Kholkin, A. L., (2009): Doping strategies for increased performance in $BiFeO_3$. *J. Magn. Magn. Mater.*, **321** (11): 1692-1698.
120. Yoneda, Y.; Sakamoto, W., (2011): Electronic and local structures of $BiFeO_3$ films. *J. Phys-Condens. Mat.*, **23** (1): 015902.
121. Qi, X.; Dho, J.; Tomov, R.; Blamire, M. G.; Macmanus-Driscoll, J. L., (2005): Greatly reduced leakage current and conduction mechanism in aliovalent-ion-doped $BiFeO_3$. *Appl. Phys. Lett.*, **86** (6): 1-3.
122. Gu, Y. H.; Wang, Y.; Chen, F.; Chan, H. L. W.; Chen, W. P., (2010): Nonstoichiometric $BiFe_{0.9}Ti_{0.05}O_3$ multiferroic ceramics with ultrahigh electrical resistivity. *J. Appl. Phy.*, **108** (9): 094112.
123. Ternon, C.; Thery, J.; Baron, T.; Ducros, C.; Sanchette, F.; Kreisel, J., (2006): Structural properties of films grown by magnetron sputtering of a $BiFeO_3$ target. *Thin Solid Films*, **515** (2): 481-484.
124. Lee, C.-C.; Wu, J.-M., (2007): Effect of film thickness on interface and electric properties of $BiFeO_3$ thin films. *Appl. Surf. Sci.*, **253** (17): 7069-7073.
125. Qi, X.; Chang, W.-C.; Kuo, J.-C.; Chen, I.-G.; Chen, Y.-C.; Ko, C.-H.; Huang, J.-C.-A., (2010): Growth and characterisation of multiferroic $BiFeO_3$ films with fully saturated ferroelectric hysteresis loops and large remanent polarisations. *J. Eur. Ceram. Soc.*, **30** (2): 283-287.
126. Zheng, R. Y.; Gao, X. S.; Zhou, Z. H.; Wang, J., (2007): Multiferroic $BiFeO_3$ thin films deposited on $SrRuO_3$ buffer layer by rf sputtering. *J. Appl. Phy.*, **101** (5): 054104.
127. Zheng, R. Y.; Sim, C. H.; Wang, J.; Ramakrishna, S., (2008): Effects of SRO Buffer Layer on Multiferroic $BiFeO_3$ Thin Films. *J. Am. Ceram. Soc.*, **91** (10): 3240-3244.
128. Lee, Y. H.; Wu, J. M.; Chueh, Y. L.; Chou, L. J., (2005): Low-temperature growth and interface characterization of $BiFeO_3$ thin films with reduced leakage current. *Appl. Phys. Lett.*, **87** (17): 172901.
129. Das, S.; Basu, S.; Mitra, S.; Chakravorty, D.; Mondal, B. N., (2010): Wet chemical route to transparent $BiFeO_3$ films on SiO_2 substrates. *Thin Solid Films*, **518** (15): 4071-4075.
130. Liu, H.; Liu, T.; Wang, X., (2009): Study on the ferroelectricity of Eu substituted films. *Solid State Commun.*, **149** (43-44): 1958-1961.
131. Wang, Y.; Nan, C. W., (2006): Enhanced ferroelectricity in Ti-doped multiferroic $BiFeO_3$ thin films. *Appl. Phys. Lett.*, **89** (5): 052903.
132. Palkar, V. R.; John, J.; Pinto, R., (2002): Observation of saturated polarization and dielectric anomaly in magnetoelectric $BiFeO_3$ thin films. *Appl. Phys. Lett.*, **80** (9): 1628.
133. Scott, J. F., (2008): Ferroelectrics go bananas. *J. Phys-Condens. Mat.*, **20** (2): 021001.
134. Eerenstein, W.; Morrison, F. D.; Dho, J.; Blamire, M. G.; Scott, J. F. A.; Mathur, N. D., (2005): Comment on ''Epitaxial $BiFeO_3$ Multiferroic Thin Film Heterostructures''. *Science*, **307**: 1203a.
135. Béa, H.; Bibes, M.; Barthélémy, A.; Bouzehouane, K.; Jacquet, E.; Khodan, A.; Contour, J. P.; Fusil, S.; Wyczisk, F.; Forget, A.; Lebeugle, D.; Colson, D.; Viret, M., (2005): Influence of parasitic phases on the properties of $BiFeO_3$ epitaxial thin films. *Appl. Phys. Lett.*, **87** (7): 072508.
136. Lahmar, A.; Zhao, K.; Habouti, S.; Dietze, M.; Solterbeck, C. H.; Es-Souni, M., (2011): Off-stoichiometry effects on $BiFeO_3$ thin films. *Solid State Ionics*, **202** (1): 1-5.
137. Ke, H.; Wang, W.; Wang, Y.; Zhang, H.; Jia, D.; Zhou, Y.; Lu, X.; Withers, P., (2012): Dependence of dielectric behavior in $BiFeO_3$ ceramics on intrinsic defects. *J. Alloys Compd.*, **541**: 94-98.
138. Lee, Y. H.; Wu, J. M.; Lai, C. H., (2006): Influence of La doping in multiferroic properties of $BiFeO_3$ thin films. *Appl. Phys. Lett.*, **88** (4): 1-3.
139. Hu, G. D.; Fan, S. H.; Yang, C. H.; Wu, W. B., (2008): Low leakage current and enhanced ferroelectric properties of Ti and Zn codoped $BiFeO_3$ thin film. *Appl. Phys. Lett.*, **92** (19): 192905.
140. Naganuma, H.; Miura, J.; Okamura, S., (2008): Ferroelectric, electrical and magnetic properties of Cr, Mn, Co, Ni, Cu added polycrystalline $BiFeO_3$ films. *Appl. Phys. Lett.*, **93** (5): 052901.
141. Chung, C. F.; Lin, J. P.; Wu, J. M., (2006): Influence of Mn and Nb dopants on electric properties of chemical-solution-deposited $BiFeO_3$ films. *Appl. Phys. Lett.*, **88** (24): 242909.
142. Simões, A. Z.; Pianno, R. F.; Aguiar, E. C.; Longo, E.; Varela, J. A., (2009): Effect of niobium dopant on fatigue characteristics of $BiFeO_3$ thin films grown on Pt electrodes. *J. Alloys Compd.*, **479** (1-2): 274-279.
143. Liu, H.; Liu, Z.; Yao, K., (2007): Improved electric properties in $BiFeO_3$ films by the doping of Ti. *J. Sol-gel Sci. Techn.*, **41** (2): 123-128.
144. Liu, H.; Liu, Z.; Yao, K., (2007): Study of the electric properties of $BiFe_{1-x}Zr_xO_{3+\delta}$ films prepared by the sol-gel process. *Physica B*, **391** (1): 103-107.
145. Yu, B.; Li, M.; Wang, J.; Pei, L.; Guo, D.; Zhao, X., (2008): Enhanced electrical properties in multiferroic $BiFeO_3$ ceramics co-doped by La^{3+} and V^{5+}. *J. Phys. D Appl. Phys.*, **41** (18): 185401.
146. Cheng, L.; Hu, G.; Jiang, B.; Yang, C.; Wu, W.; Fan, S., (2010): Enhanced piezoelectric properties of epitaxial W-Doped $BiFeO_3$ thin films. *Appl. Phys. Express*, **3** (10): 101501.
147. Singh, S. K.; Ishiwara, H.; Maruyama, K., (2006): Room temperature ferroelectric properties of Mn-substituted $BiFeO_3$ thin films deposited on Pt electrodes using chemical solution deposition. *Appl. Phys. Lett.*, **88** (26): 262908.
148. Wen, Z.; Hu, G.; Fan, S.; Yang, C.; Wu, W.; Zhou, Y.; Chen, X.; Cui, S., (2009): Effects of annealing process and Mn substitution on structure and ferroelectric properties of $BiFeO_3$ films. *Thin Solid Films*, **517** (16): 4497-4501.
149. Zhang, S. T.; Lu, M. H.; Wu, D.; Chen, Y. F.; Ming, N. B., (2005): Larger polarization and weak ferromagnetism in quenched $BiFeO_3$ ceramics with a distorted rhombohedral crystal structure. *Appl. Phys. Lett.*, **87** (26): 1-3.
150. Das, R. R.; Kim, D. M.; Baek, S. H.; Eom, C. B.; Zavaliche, F.; Yang, S. Y.; Ramesh, R.; Chen, Y. B.; Pan, X. Q.; Ke, X.; Rzchowski, M. S.; Streiffer, S. K., (2006): Synthesis and ferroelectric properties of epitaxial $BiFeO_3$ thin films grown by sputtering. *Appl. Phys. Lett.*, **88** (24): 242904.
151. Wu, J.; Wang, J.; Xiao, D.; Zhu, J., (2011): Resistive hysteresis in $BiFeO_3$ thin films. *Mater. Res. Bull.*, **46** (11): 2183-2186.
152. Yun, K. Y., (2004): Giant ferroelectric polarization beyond 150 $\mu C/cm^2$ in $BiFeO_3$ thin film. *Jpn. J. Appl. Phys.*, **43** (5 A): L647-L648.
153. Yun, K. Y.; Noda, M.; Okuyama, M., (2003): Prominent ferroelectricity of $BiFeO_3$ thin films prepared by pulsed-laser deposition. *Applied Physics Letters*, **83** (19): 3981-3983.
154. Ueda, K.; Tabata, H.; Kawai, T., (1999): Coexistence of ferroelectricity and ferromagnetism in $BiFeO_3$-$BaTiO_3$ thin films at room temperature. *Applied Physics Letters*, **75** (4): 555-557.
155. Teague, J. R.; Gerson, R.; James, W. J., (1970): Dielectric Hysteresis in Single Crystal $BiFeO_3$. *Solid State Commun.*, **8** (13): 1073-1074.
156. Ederer, C.; Spaldin, N. A., (2005): Influence of strain and oxygen vacancies on the magnetoelectric properties of multiferroic bismuth ferrite. *Phys. Rev. B*, **71** (22): 224103.
157. Bai, F.; Wang, J.; Wuttig, M.; Li, J.; Wang, N.; Pyatakov, A. P.; Zvezdin, A. K.; Cross, L. E.; Viehland, D., (2005): Destruction of spin cycloid in (111)c -oriented $BiFeO_3$ thin films by epitiaxial constraint: Enhanced polarization and release of latent magnetization. *Appl. Phys. Lett.*, **86** (3): 1-3.
158. Mazumder, R.; Sujatha Devi, P.; Bhattacharya, D.; Choudhury, P.; Sen, A.; Raja, M., (2007): Ferromagnetism in nanoscale $BiFeO_3$. *Appl. Phys. Lett.*, **91** (6): 062510.
159. Park, T. J.; Papaefthymiou, G. C.; Viescas, A. J.; Moodenbaugh, A. R.; Wong, S. S., (2007): Size-dependent magnetic properties of single-crystalline multiferroic $BiFeO_3$ nanoparticles. *Nano Lett.*, **7** (3): 766-772.
160. Jaiswal, A.; Das, R.; Vivekanand, K.; Abraham, P. M.; Adyanthaya, S.; Poddar, P., (2010): Effect of reduced particle size on the magnetic properties of chemically synthesized $BiFeO_3$ nanocrystals. *J. Phys. Chem. C*, **114** (5): 2108-2115.
161. Annapu Reddy, V.; Pathak, N. P.; Nath, R., (2013): Particle size dependent magnetic properties and phase transitions in multiferroic $BiFeO_3$ nanoparticles. *J. Alloys Compd.*, **543**: 206-212.
162. Vijayanand, S.; Mahajan, M. B.; Potdar, H. S.; Joy, P. A., (2009): Magnetic characteristics of nanocrystalline multiferroic $BiFeO_3$ at low temperatures. *Phys. Rev. B*, **80** (6): 064423.
163. Khomchenko, V. A.; Kiselev, D. A.; Vieira, J. M.; Jian, L.; Kholkin, A. L.; Lopes, A. M. L.; Pogorelov, Y. G.; Araujo, J. P.; Maglione, M., (2008): Effect of diamagnetic Ca, Sr, Pb, and Ba substitution on the crystal structure and multiferroic properties of the $BiFeO_3$ perovskite. *J. Appl. Phy.*, **103** (2): 024105.
164. Singh, P.; Jung, J. H., (2010): Effect of oxygen annealing on magnetic, electric and magnetodielectric properties of Ba-doped $BiFeO_3$. *Physica B*, **405** (4): 1086-1089.
165. Cheng, Z. X.; Wang, X. L.; Du, Y.; Dou, S. X., (2010): A way to enhance the magnetic moment of multiferroic bismuth ferrite. *J. Phys. D Appl. Phys.*, **43** (24): 242001.
166. Troyanchuk, I. O.; Tereshko, N. V.; Chobot, A. N.; Bushinsky, M. V.; Bärner, K., (2009): Weak ferromagnetism in $BiFeO_3$ doped with titanium. *Physica B*, **404** (21): 4185-4189.
167. Singh, H.; Yadav, K. L., (2012): Effect of Nb substitution on the structural, dielectric and magnetic properties of multiferroic $BiFe_{1-x}Nb_xO_3$ ceramics. *Mater. Chem. Phys.*, **132** (1): 17-21.
168. Wei, J.; Haumont, R.; Jarrier, R.; Berhtet, P.; Dkhil, B., (2010): Nonmagnetic Fe-site doping of $BiFeO_3$ multiferroic ceramics. *Appl. Phys. Lett.*, **96** (10): 102509.

Recibido: 28/09/2013
Recibida versión corregida: 20/12/2013
Aceptado: 20/12/2013